In presenting the dissertation as a partial fulfillment of the requirements for an advanced degree from the Georgia Institute of Technology, I agree that the Library of the Institute shall make it available for inspection and circulation in accordance with its regulations governing materials of this type. I agree that permission to copy from, or to publish from, this dissertation may be granted by the professor under whose direction it was written, or, in his absence, by the Dean of the Graduate Division when such copying or publication is solely for scholarly purposes and does not involve potential financial gain. It is understood that any copying from, or publication of, this dissertation which involves potential financial gain will not be allowed without written permission.

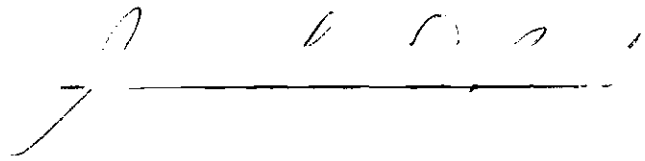

3/17/65
b

STUDY OF A BETA-GAMMA DIRECTIONAL CORRELATION IN THE DECAY OF Sb^{125}

A THESIS

Presented to

The Faculty of the Graduate Division

by

James Leroy DuBard

In Partial Fulfillment

of the Requirements for the Degree

Doctor of Philosophy in the School of Physics

Georgia Institute of Technology

May, 1966

STUDY OF A BETA-GAMMA DIRECTIONAL CORRELATION

IN THE DECAY OF Sb^{125}

Approved:

Chairman

Date approved by Chairman:

ACKNOWLEDGMENTS

The author wishes to express his deep appreciation for the influence of Dr. L. D. Wyly, Jr. and Dr. Charles H. Braden throughout his graduate study in physics. They suggested the topic for the thesis research and gave personal guidance and assistance during the research. A debt of gratitude is also owed Dr. E. T. Patronis, Jr. and Mr. N. S. Kendrick who designed, constructed, and maintained the electronic equipment used in the research and who assisted the author in innumerable ways. A fellowship from the National Aeronautics and Space Administration made possible three years of concentrated graduate study. The thesis research was supported in part by the National Science Foundation. Finally, the author must humbly acknowledge the constant, unquestioning love and support of his wife during six years of marriage to a student.

TABLE OF CONTENTS

Page

ACKNOWLEDGMENTS ii

LIST OF TABLES. v

LIST OF ILLUSTRATIONS vi

SUMMARY vii

Chapter

I. INTRODUCTION 1

The Role of Directional Correlation Studies. 1
The Sb^{125} Problem. 4
Preliminary Studies. 7

II. EXPERIMENTAL APPARATUS 9

III. PROPERTIES OF THE MAGNETIC LENS. 14

Analysis of Focusing Parameters. 14
Measurement of Focusing Parameters 15

IV. MEASUREMENT OF THE DIRECTIONAL CORRELATION 21

V. ANALYSIS OF THE BETA TRANSITION. 30

Analysis of the Intermediate State Spin. 30
Nuclear Model Predictions. 32
Analysis of the Nuclear Matrix Elements. 33

VI. RECOMMENDATIONS FOR FUTURE RESEARCH. 42

APPENDICES. 44

A. FOCAL LENGTHS AND PRINCIPAL PLANES OF A MAGNETIC QUADRUPOLE 45

TABLE OF CONTENTS (Concluded)

Page

B. OUTLINE OF THE THEORETICAL FORMALISM 51

The Beta Decay Transition. 51
The Beta-Gamma Directional Correlation 54

C. ANALYSIS OF EXPERIMENTAL DATA. 59

D. ANGULAR RESOLUTION CORRECTION. 65

BIBLIOGRAPHY. 70

VITA. 73

LIST OF TABLES

Table		Page
1.	Sb^{125} Directional Correlation Data for the 0.295 MeV Beta Group and the 0.427 MeV Gamma	26
2.	Sb^{125} Directional Correlation Data for the 0.437 MeV Beta Group and the 0.176 MeV Gamma	26
3.	Beta Decay Transitions	53
4.	Analysis of Data for the Directional Correlation of Beta Rays in the Energy Range 0.235 - 0.275 MeV and the 0.176 MeV Gamma	62

LIST OF ILLUSTRATIONS

Figure		Page
1.	Decay Scheme of Sb^{125}	5
2.	Top View Schematic of Experimental Apparatus	10
3.	Photograph of Experimental Apparatus	11
4.	Block Diagram of Electronic Equipment	13
5.	Maximum Beta Counting Rate versus Source-to-Detector Distance	18
6.	Electron Energy versus Quadrupole Focusing Currents	20
7.	Sb^{125} Gamma Ray Spectrum	23
8.	Experimental Directional Correlation A_2 Coefficient	27
9.	Gamma Coincidence Spectrum with the 0.437 MeV Beta Group	28
10.	Gamma Coincidence Spectrum with the 0.437 and 0.295 Mev Beta Groups	29
11.	Theoretical Directional Correlation A_2 Coefficient for $J_1 = 11/2$	31
12 a.	Nuclear Matrix Element Parameters Consistent with the Experimental A_2 Coefficient	36
12 b.		37
12 c.		38
13.	Theoretical Directional Correlation A_2 Coefficient for $J_1 = 9/2$	40
14.	Ratio of the Shape Correction Factors at Beta Energies 0.410 MeV and 0.287 MeV	41
15.	Electron Trajectories in a Magnetic Quadrupole	47
16.	Geometry for Angular Resolution Correction	67

SUMMARY

The decay scheme of Sb^{125} has been extensively investigated with results in good agreement for the low-lying states of the daughter Te^{125}. The spin of the ground state and first two excited states has been established along with the multipolarity of the connecting gamma transitions. The spin of the third excited state, 0.321 MeV above the ground state, has been restricted to be either 9/2 or 11/2. The 0.321 MeV state is populated by a first-forbidden beta transition of end-point energy 0.437 MeV in the decay of Sb^{125}. The state is depopulated by a 0.176 MeV gamma transition found to be a mixture of M1 and E2 radiations. The mixing ratio is not known. The present research centered on the measurement of the directional correlation of the 0.437 MeV beta group and the 0.176 MeV gamma ray for the purpose of determining the spin of the 0.321 MeV state in Te^{125}. The experimental data were further used to analyze the relative magnitudes of the nuclear matrix elements of the beta decay interaction Hamiltonian operative for the first-forbidden 0.437 MeV beta transition.

The experimental setup consisted of a fixed beta detector and a gamma detector moveable about the radioactive source so that the angle between the trajectories of the beta and gamma radiations was variable from 90 degrees to 270 degrees. A 1.5 inch diameter by one inch thick sodium iodide (thallium activated) scintillation crystal was used for gamma detection, and a 1.5 inch diameter by two millimeter thick anthracene scintillation crystal was used for beta detection. The two detectors fed into single channel pulse height analyzers and a fast-slow coincidence

circuit set for a resolving time of about 55 nanoseconds.

The initial coincidence studies revealed a highly asymmetric gamma-gamma coincidence background due to Compton scattering of gamma rays from several intense gamma transitions of energy about 0.600 MeV in the decay of Sb^{125}. A Compton event in one detector followed by detection of the scattered gamma ray in the other detector produced absorbed energies in the range of the beta-gamma transition energies under investigation. This gamma-gamma background was eliminated by greatly increasing the source-to-detector distance for the beta rays, thereby decreasing the gamma ray intensity at the beta detector by the inverse-square-law effect. A pair of quadrupole magnets was used to focus the beta rays. Extensive investigation of the behavior of the magnetic quadrupole lens led to the adoption of an object distance of four centimeters and an image distance of 25.6 centimeters, measured from the respective faces of the lens. The total distance from the source to the beta detector was 60 centimeters. The effective source-to-detector distance was found to be about 23 centimeters by comparing the counting rate with that for a simple geometry. The focusing currents required in the two quadrupole magnets were determined by maximizing the counting rate for several monoenergetic electron sources. Calibration plots of focusing current versus electron energy were obtained using the conversion lines of Cs^{137} and Sn^{113} and the L conversion line of Hg^{203}. The focusing currents were such that the magnetic field at the pole faces was in the range 80 to 200 gauss.

The directional correlation of the allowed 0.295 MeV beta group and the 0.427 MeV gamma ray, in the decay of Sb^{125}, was measured as a final check of instrumental asymmetries. The correlation was found to be iso-

tropic. The directional correlation of the 0.437 MeV beta group and the 0.176 MeV gamma ray was measured at four beta energies in the range 0.255 to 0.410 MeV. The correlation is conventionally expressed as

$$N(\theta) = 1 + A_2 P_2(\cos \theta) \ .$$

The calculated A_2 coefficients, corresponding to the weighted average of several measurements at each beta energy, were as follows:

Beta Energy	A_2 Coefficient	Probable Error
0.255 MeV	0.100	0.009
0.305 MeV	0.132	0.009
0.355 MeV	0.185	0.008
0.410 MeV	0.211	0.011

The A_2 coefficient was found to increase rapidly and monotonically with beta energy.

The 0.437 MeV beta transition involves a nuclear spin change of two units under the assumption of spin 11/2 for the 0.321 MeV state in Te^{125}. In this case, the theoretical beta energy dependence of the A_2 coefficient is unambiguously calculable. Disagreement of the calculated energy dependence with experimental results led to the conclusion that the spin of the 0.321 MeV state is 9/2.

The theoretical A_2 coefficient may be formulated in terms of the

gamma multipole mixing ratio δ and three parameters Υ, x, and u, representing ratios of the several operative nuclear matrix elements. The ratio of the theoretical A_2 coefficients at two different beta energies is independent of δ. Using the ratio of the experimental A_2 coefficients at two different beta energies and a range of independent variables Υ and x, a fourth-order equation in the parameter u was solved by use of a digital computer. Using the experimental A_2 coefficient at one beta energy and a set of values Υ, x, and u, a quadratic equation in the mixing ratio δ was solved. The parameters x and u were bounded away from zero in all solutions consistent with the experimental energy dependence of the A_2 coefficient. The parameter Υ exhibited a forbidden range from about 0.6 to 1.6. It has been estimated in the literature that conventional beta decay theory should give a value for Υ about 0.94 for this beta transition while the conserved vector current theory should give a value about 2.34. Every pair of solutions for the gamma multipole mixing ratio δ contained one value indicating a predominantly M1 transition and the other value indicating a predominantly E2 transition.

CHAPTER I

INTRODUCTION

The Role of Directional Correlation Studies

The direction of emission of a nuclear radiation relative to a laboratory coordinate system depends in general on the orientation of the nuclear spin relative to that coordinate system (1). The radiations from a large population of radioactive nuclei will generally be isotropic in direction due to random orientations of the nuclear spins. However, the observation of nuclear radiations in a fixed spatial direction selects a subpopulation of radioactive nuclei having their nuclear spins preferentially oriented with respect to the direction of the observed radiations. Then the direction of emission of a second radiation, in immediate succession to the first radiation, will show a correlation with the direction of emission of the first radiation. That is, the probability of emission of the two successive radiations depends in general on the angle between the two directions of emission. This directional correlation phenomenon is included in the term angular correlation which may indicate the observation of the linear or circular polarization of either of the radiations in addition to the two directions of emission.

The first theoretical investigation of the angular correlation between two successively emitted gamma rays was published by Hamilton in 1940 (2). The early efforts to verify experimentally the predictions of Hamilton's theory were unsuccessful due to inadequate equipment and tech-

nique. The first successful angular correlation measurements were performed by Brady and Deutsch in 1947 using Geiger counters for radiation detection (3). During the next three years these researchers began using scintillation counters which gave great improvement in counting efficiency, counting speed, and energy sensitivity. Frauenfelder gave a review in 1953 of these early angular correlation experiments and an elementary formulation of the theory (4). In the same year, Biedenharn and Rose published a complete theory of the angular correlations of nuclear radiations (5).

Before the original work in angular correlation theory, considerable work had been done toward formulating the theory of the beta decay interaction. In 1941, Konopinski and Uhlenbeck published a review of the theory of forbidden beta transitions that established a standard for the formalism (6). Interest in beta-gamma angular correlation studies was greatly stimulated by the prediction (7) and experimental verification (8) of nonconservation of parity in the beta decay interaction. Subsequent to this discovery, reviews of the theory of the beta-decay interaction were published by Konopinski (9), for allowed transitions, and by Weidenmüller (10), for forbidden transitions. A recent textbook treatment of the theory has been given by Preston (11). The theory of beta-gamma angular correlations is greatly complicated by contributions from various nuclear matrix elements of the Hamiltonian which describes the beta decay interaction. Only recently has the theory been put into forms which may easily be compared with experimental results. Kotani and Ross (12) and Kotani (13) have given formulas for first-forbidden beta-gamma angular correlations using an approximation established by Konopinski and Uhlenbeck (6). In this approximation, the finite size of the nuclear charge distribution is neglected.

The electron wave function is evaluated at the nuclear surface and taken outside the matrix element integral over the nuclear volume. The electron wave function is then expanded in terms of the nuclear radius, neglecting terms of order $(\alpha Z)^2$, where α is the fine structure constant and Z is the atomic number. Newsome and Fischbeck have shown that this approximation is not always satisfactory (14). Bhalla and Rose have made exact numerical calculations of the electron wave function, evaluated at the nuclear surface, for a wide range of atomic number and electron energy (15) (16). These calculations include the effect of finite nuclear size. These exact electron functions are used explicitly in the formulas of Morita and Morita for the beta-gamma angular correlation (17). The salient features of the theory used to analyze the beta and gamma transitions are outlined in Appendix B.

In general, the beta-gamma angular correlation may be theoretically formulated as the sum of a finite series of Legendre polynomials (1) (17). The coefficients of the Legendre polynomials depend on the various observables, such as energy and angular momentum, of the nuclear states involved in the transitions and of the emitted radiations. Furthermore, the coefficients depend on the nuclear matrix elements of various terms in the Hamiltonian which describes the beta decay interaction. If some of the observables are known from other independent measurements, then a comparison of angular correlation theory and experiment may serve to determine the remaining unknown observables. This comparison of theory and experiment may also indicate the relative magnitudes of the various nuclear matrix elements. Thus angular correlation studies serve as a basic tool of the nuclear physicist for gaining insight into nuclear structure and

nuclear interactions. This information is used in turn to evaluate the effectiveness of various nuclear models in the continuing search for a comprehensive theory of the behavior of the atomic nucleus.

The Sb^{125} Problem

The ground state of Sb^{125} is predicted to be a $\frac{7}{2}$ + state by the single-particle model for one proton outside a closed shell of 50 protons (18). This spin assignment is compatible with the measurements of Burson (19) and Arya and Nicholson (20) on the decay scheme of Sn^{125}. The decay scheme of Sb^{125} has been studied by several researchers (21) (22) (23) (24) (25) with results in good agreement for the low-lying excited states of Te^{125}. This decay scheme is given in Figure 1 (26). The ground state spin of Te^{125} has been established as $\frac{1}{2}$ from measurements of the hyperfine structure in the spectrum of singly-ionized Te^{125} (27).

Measurements of conversion coefficients and conversion ratios for various gamma transitions in the decay of Sb^{125} have determined the multipolarity of some of these gamma rays and thereby the spin and parity of some of the excited states in Te^{125} (25) (28). The conservation of angular momentum between the initial and final nuclear states and the gamma ray establishes a triangle inequality between the respective angular momentum quantum numbers (29). $|J_i - J_f| \leq L \leq J_i + J_f$, where L is the angular momentum quantum number of the gamma multipole of order L connecting the initial and final nuclear states. The angular momentum quantum number J is referred to as the spin of a nuclear state. The gamma multipole also establishes a definite relationship between the parities of the initial and final nuclear states (29). The ratio of these parities equals

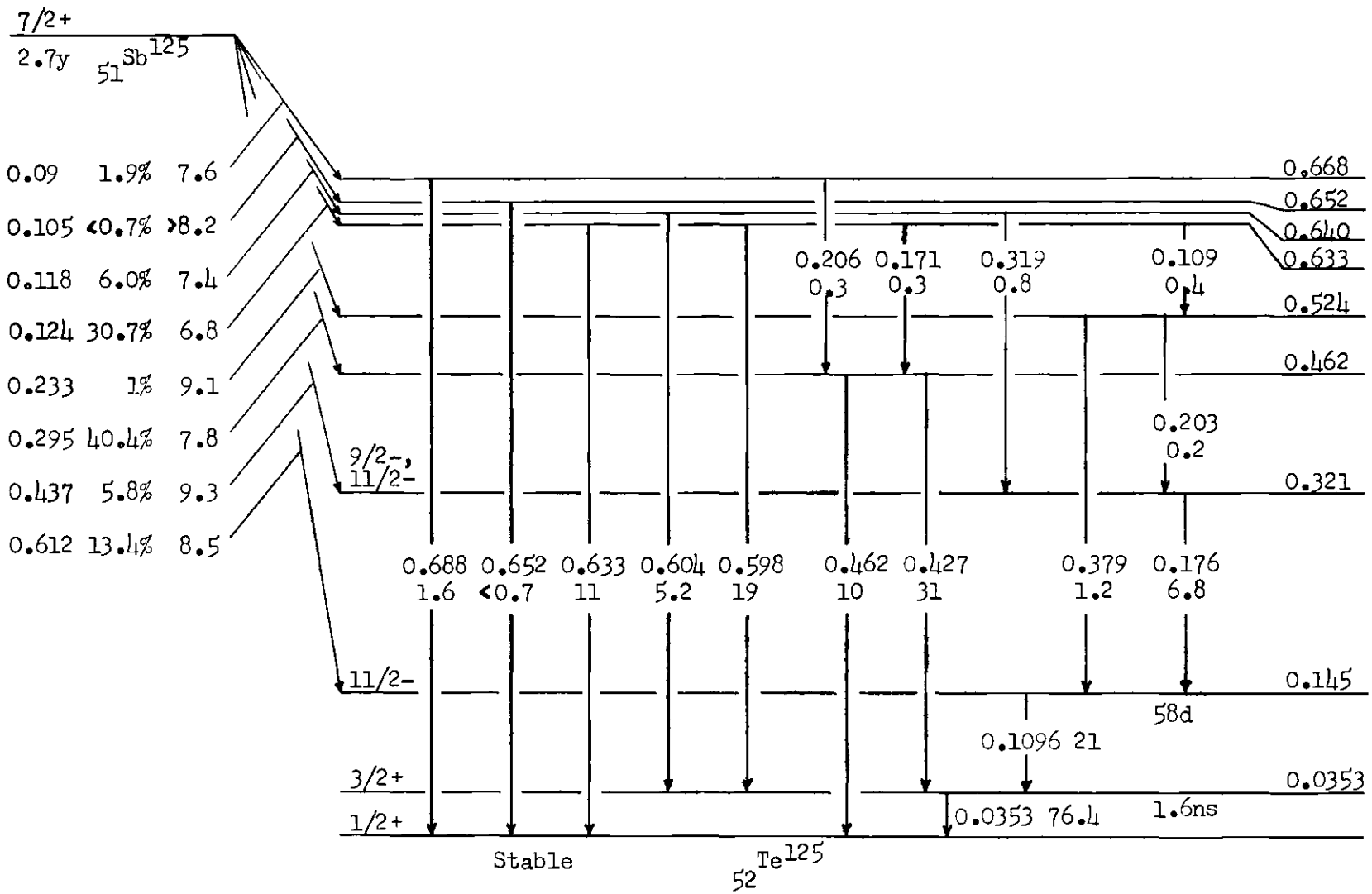

Figure 1. Decay Scheme of Sb^{125}.

$(-1)^L$ for electric multipole radiation of order L, denoted as EL. The sign is opposite for magnetic multipole radiation of the same order, denoted as ML.

The 0.0353 MeV gamma transition has been found to be M1 radiation (25) (28). Conservation of angular momentum and parity permit the 0.0353 MeV excited state in Te^{125} to have a spin of either 1/2 or 3/2 and the same parity as the ground state. The 0.0353 MeV state in Te^{125} is reached by an electron capture transition from the 5/2+ ground state of I^{125}. A $\log_{10}$ ft value of 4.9 identifies this transition as allowed, with the spin change selection rule $\Delta J = 0$ or ± 1. Therefore, the spin of the 0.0353 MeV state in Te^{125} must be 3/2.

The 0.1096 MeV gamma transition has been found to be M4 radiation (25). The 0.145 MeV state in Te^{125} must have a spin of 11/2 and parity opposite to that of the ground state. A lower spin assignment would give high probability for deexcitation by a gamma multipole of order three with conversion ratios much different from those observed. The 0.145 MeV state in Te^{125} is a 58 day isomeric state.

Narcisi has interpreted his data to require that the 0.176 MeV gamma transition be a mixture of M1 and E2 radiations (25). The presence of M1 radiation limits the spin of the 0.321 MeV state in Te^{125} to values 13/2, 11/2, or 9/2. The 0.321 MeV state has the same parity as the 0.145 MeV state. The $\log_{10}$ ft value of the 0.437 MeV beta group which feeds the 0.321 MeV state is 9.3. This $\log_{10}$ ft value indicates a first-forbidden beta transition having the spin change selection rule $\Delta J = 0, \pm 1$, or ± 2 and giving a change in parity. Since the Sb^{125} ground state is 7/2+, the 0.321 MeV state in Te^{125} must be either 9/2 - or 11/2 -. Narcisi has

chosen the assignment 9/2 - to achieve internal consistency in his decay scheme. On the other hand, the measurements of Inamura, et al, indicated the 11/2 - assignment (30).

For the 0.176 MeV gamma transition, Narcisi measured a K conversion coefficient of 0.156 and a K to L conversion ratio greater than 5.45 (25). The conversion coefficient tables of Rose give a K conversion coefficient of 0.18 and a K to L conversion ratio of 4.72 for a pure E2 gamma transition of energy 0.176 MeV (31). Consideration of the magnitude of error commonly encountered in conversion coefficient measurements and allowance for some margin of error due to approximations made in the theoretical calculations indicate that a pure E2 multipole assignment for the 0.176 MeV gamma ray cannot be ruled out. If this transition is pure E2, then the spin of the 0.321 MeV state in Te^{125} can be 7/2; in which case, the absence of any spin change in the 0.437 MeV beta transition greatly complicates the theoretical analysis of this transition.

The purpose of the present research is to measure the beta-gamma directional correlation for the 0.437 MeV beta group, in the decay of Sb^{125}, in coincidence with the 0.176 MeV gamma ray in hope of determining the spin of the 0.321 MeV level in Te^{125} and establishing some limitations on the relative magnitudes of the nuclear matrix elements of the beta decay interaction Hamiltonian.

Preliminary Studies

The first efforts to measure the beta-gamma directional correlation for the 0.437 MeV beta group in coincidence with the 0.176 MeV gamma ray revealed a highly asymmetric gamma-gamma coincidence background due to

Compton scattering of gamma rays from the several intense gamma transitions at about 0.600 MeV. A Compton event in one radiation detector followed by detection of the scattered gamma ray in the other radiation detector produced absorbed energies in the range of the beta-gamma transition energies under investigation. No shielding technique was found to be adequate to eliminate this effect when the radiation detectors were set to detect beta rays and gamma rays emitted at a relative angle of 180 degrees. It was decided to try increasing greatly the source-to-detector distance for the beta rays, thereby decreasing the gamma ray intensity at the beta detector by the inverse-square-law effect. At the same time, a means was sought to maintain the beta ray intensity at the beta detector by magnetically focusing the beta rays. A pair of magnetic quadrupoles was chosen for this purpose.

CHAPTER II

EXPERIMENTAL APPARATUS

The lens used to focus the beta rays was a pair of magnetic quadrupoles, Model 1005, manufactured by Spectromagnetic Industries. The aperture between magnetic pole faces was 2.01 inches, and the length of the pole faces was four inches. The magnetic field at the pole faces was rated by the manufacturer to be 790 gauss for a coil current of eight amperes. The magnetization curve supplied by the manufacturer was linear from zero to eight amperes. The two quadrupoles were mounted on aluminum supports with a separation of seven inches between centers. A schematic diagram of the experimental setup is given in Figure 2, and a photograph is given in Figure 3.

The vacuum chamber was constructed from aluminum stock. The radioactive source was contained in the cylindrical cup protruding from the face of the magnetic quadrupole in the foreground of Figure 3. This cup was fitted onto the end of a two inch outer diameter pipe which extended through the aperture of the magnetic lens into a housing for the beta detector. This housing was a telescoping arrangement to provide fine adjustments, set by spacing rings, in the image distance of the lens. Various lengths of two inch pipe were cut to provide coarse adjustments in object and image distance. All joints were fitted with O-ring seals. The operating pressure in the chamber was about ten microns of mercury.

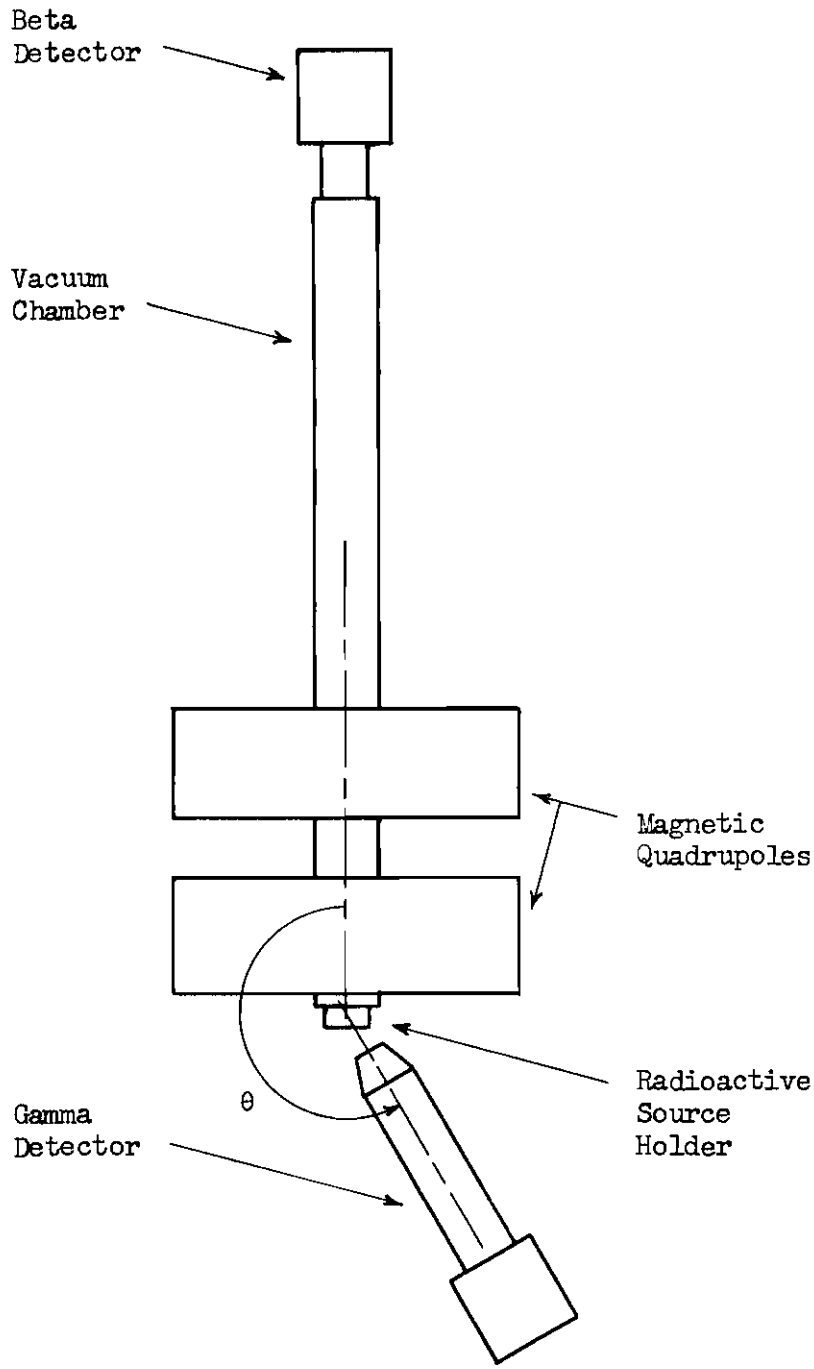

Figure 2. Top View Schematic of Experimental Apparatus.

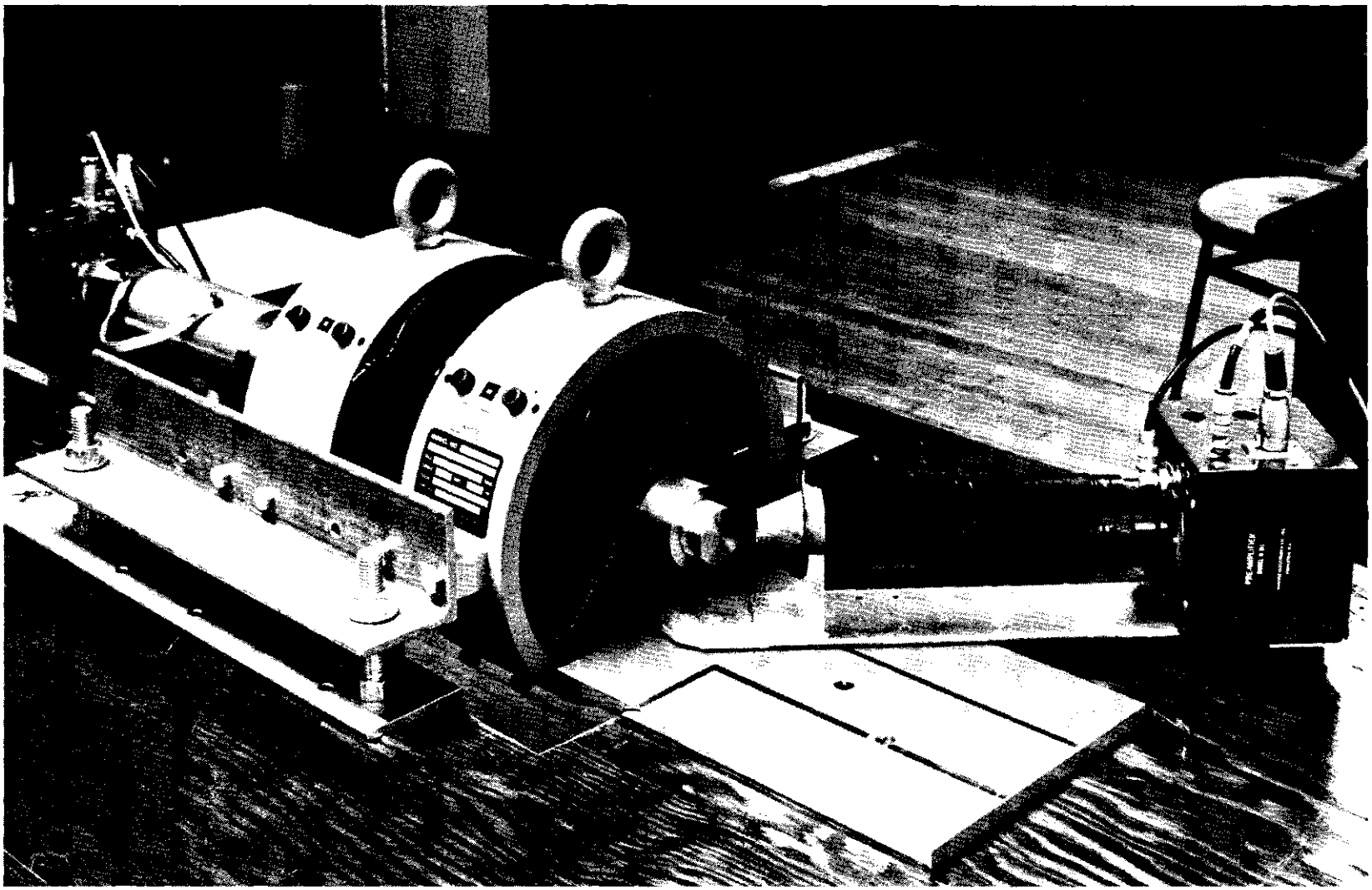

Figure 3. Photograph of Experimental Apparatus.

A 1.5 inch diameter by one inch thick sodium iodide (thallium activated) scintillation crystal was used for gamma detection, and a 1.5 inch diameter by two millimeter thick anthracene scintillation crystal was used for beta detection. The scintillation crystals were mounted on RCA 6655-A photomultiplier tubes fitted into preamplifiers. The gamma detector was moveable about the radioactive source so that the angle θ between the trajectories of the beta and gamma radiations, as shown in Figure 2, was variable from 90 degrees to 270 degrees. The gamma detector was positioned six centimeters from the source, subtending a geometrical solid angle of 0.29 steradian. The two detectors fed into pulse height analyzers and a fast-slow coincidence circuit set for a resolving time of about 55 nanoseconds. A block diagram of the electronic equipment is given in Figure 4. A Hamner Model N220 scaler was used to count triple coincidences. All other electronic equipment was designed and built by Dr. E. T. Patronis and Mr. N. S. Kendrick.

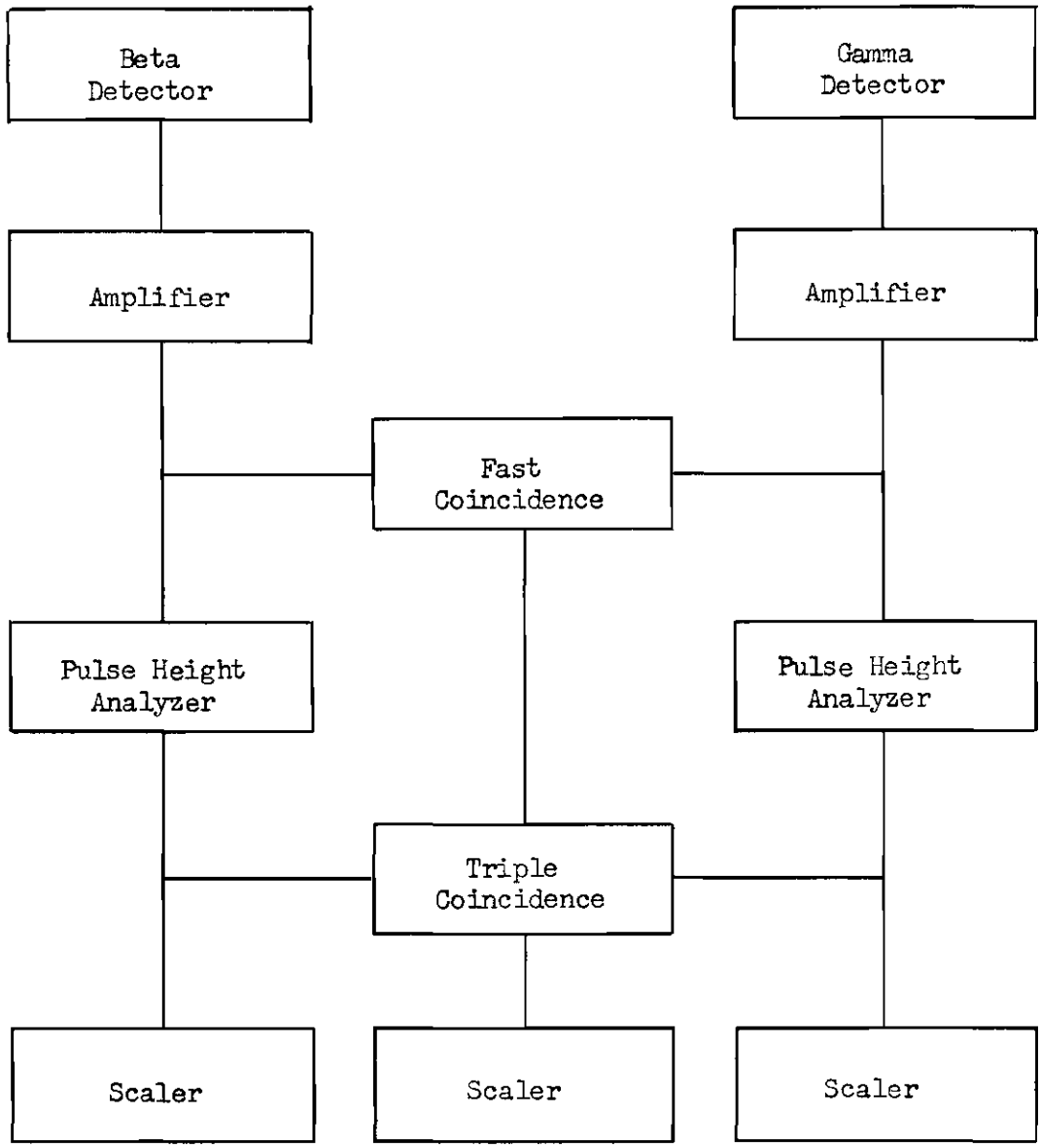

Figure 4. Block Diagram of Electronic Equipment.

CHAPTER III

PROPERTIES OF THE MAGNETIC LENS

Analysis of Focusing Parameters

The path of motion of an electron in the field of a magnetic quadrupole is easily obtained under certain simplifying conditions (32)(33)(34). The analysis of electron trajectories is outlined in Appendix A. The magnetic field as a function of distance along a line parallel to the z axis through the center of the quadrupole is assumed to be a step function of constant magnitude over an "effective length" of the quadrupole specified by the manufacturer. The x or y displacement of an electron incident parallel to the z axis is found to be a cosine or hyperbolic cosine function of the distance along z in the converging or diverging plane, respectively. The linear path of motion of this electron, outside the magnetic field, intersects the z axis at the focal length of the magnetic lens, leading to expressions for the object and image distances relative to the principal planes of the lens.

Expressions for the object and image distances relative to the external faces of a compound lens, consisting of a pair of magnetic quadrupoles with reversed polarities, were programmed for the Burroughs B5500 computer at the Rich Electronic Computer Center in order to examine the feasibility of using this lens for the directional correlation measurement. The computer calculated the image distances and magnifications in two orthogonal planes for a wide range of object distance and magnetic field

gradient. The magnetic field at the pole face was related to current in the coil winding by a magnetization curve supplied by the manufacturer. The calculations yielded a small number of combinations of magnetic lens parameters resulting in a non-astigmatic focus. In such cases, the ratio of the magnification in two orthogonal planes was found to be of the order of ten or twenty to one. The calculations were found to be very sensitive to slight changes in the focusing parameters.

Measurement of Focusing Parameters

Monoenergetic conversion electrons from the decay of Cs^{137}, Sn^{113}, and Hg^{203} were used to study the behavior of the magnetic lens. Cs^{137} and Sn^{113} were obtained as chlorides in hydrochloric acid solution and Hg^{203} as a nitrate in nitric acid solution from the Oak Ridge National Laboratory. Radioactive sources were prepared by evaporating successive drops of the solution on a 0.25 mil clear mylar sheet glued over the face of a shallow lucite cylinder. The crystalline residue was thinly coated with a clear plastic spray. The other face of the lucite cylinder was also covered with mylar; so the source was completely encapsulated except for a small pump-out hole. The source was electrically grounded through an aquadag path. The diameter of various sources prepared ranged from two to four millimeters. The 0.624 MeV and 0.365 MeV conversion lines from the decay of Cs^{137} and Sn^{113}, respectively, were well resolved. The L conversion line of Hg^{203} at about 0.264 MeV was poorly resolved, and the actual location of this line with reference to the pulse height analyzer setting was determined by fitting a gaussian curve to the tail of the electron energy spectrum. This source was used only in the final energy calibration, Figure 6.

Magnetizing currents in the two quadrupoles were varied to maximize the electron counting rate, using a combination of object and image distances for a non-astigmatic focus as determined by the computer analysis. With the pulse height analyzer set to accept the conversion electron line, the electron counting rate was observed as one current was increased monotonically while the second current was held constant. Then the iron cores were demagnetized, using a variac, to eliminate hysteresis effects. The process was repeated with the first current maintained constant at a value corresponding to maximum electron counting rate on the previous trial. The iteration was continued to a point of convergence. This iteration procedure was used repeatedly for many weeks and the iteration was begun at different points to show that the procedure would in fact converge and that the point of convergence was reproducible.

The focusing currents determined experimentally for a given combination of object and image distances did not agree with those specified by computer analysis of electron trajectories based on the manufacturer's specifications for the magnets. Aside from the effect of any error in these specifications, this disagreement was due to a difference in the definition of focusing currents. The experimental procedure of maximizing the counting rate attained a maximum flux of electrons over the area of the scintillation crystal. This result involved an interplay between conditions determining a non-astigmatic image and conditions determining the magnification of the image. Maximum transmission of electrons from source to detector was the criterion of importance for application to the directional correlation measurement, and the analysis of electron trajectories was not pursued. For a given object distance, the maximum elec-

tron counting rate was found to decrease monotonically with increasing image distance. This result is plotted in Figure 5. The choice of focusing parameters had to be a compromise between small source-to-detector distance for high electron transmission and large source-to-detector distance to reduce the gamma ray intensity at the electron detector.

Photographs of the distribution of electron intensity over the area of the scintillation crystal were taken for various combinations of object and image distances using photographic film packets designed for personnel radiation monitoring. A two-millimeter-diameter Sn^{113} source was prepared with sufficient activity to give a good photographic image with one hour exposure time. The experimental data, together with the requirement for an object distance large enough to permit proper positioning of the gamma detector, led to the final choice of an object distance of 4 centimeters and an image distance of 25.6 centimeters measured from the respective faces of the lens. The total source-to-detector distance was 60 centimeters. The resulting electron distribution over the area of the scintillation crystal was confined to a band about 0.5 centimeter wide. The remaining area of the scintillation crystal was masked with a thick, lucite-lined, lead shield to further eliminate gamma rays.

The solid angle subtended by the beta detector depended in a complicated way upon the possible electron trajectories through the magnetic lens. Although such a lens would focus rather widely divergent electrons moving precisely in the converging plane of the first quadrupole, this angle of divergence was in fact limited to less than 15 degrees by the inner diameter of the aluminum pipe forming the evacuated path through

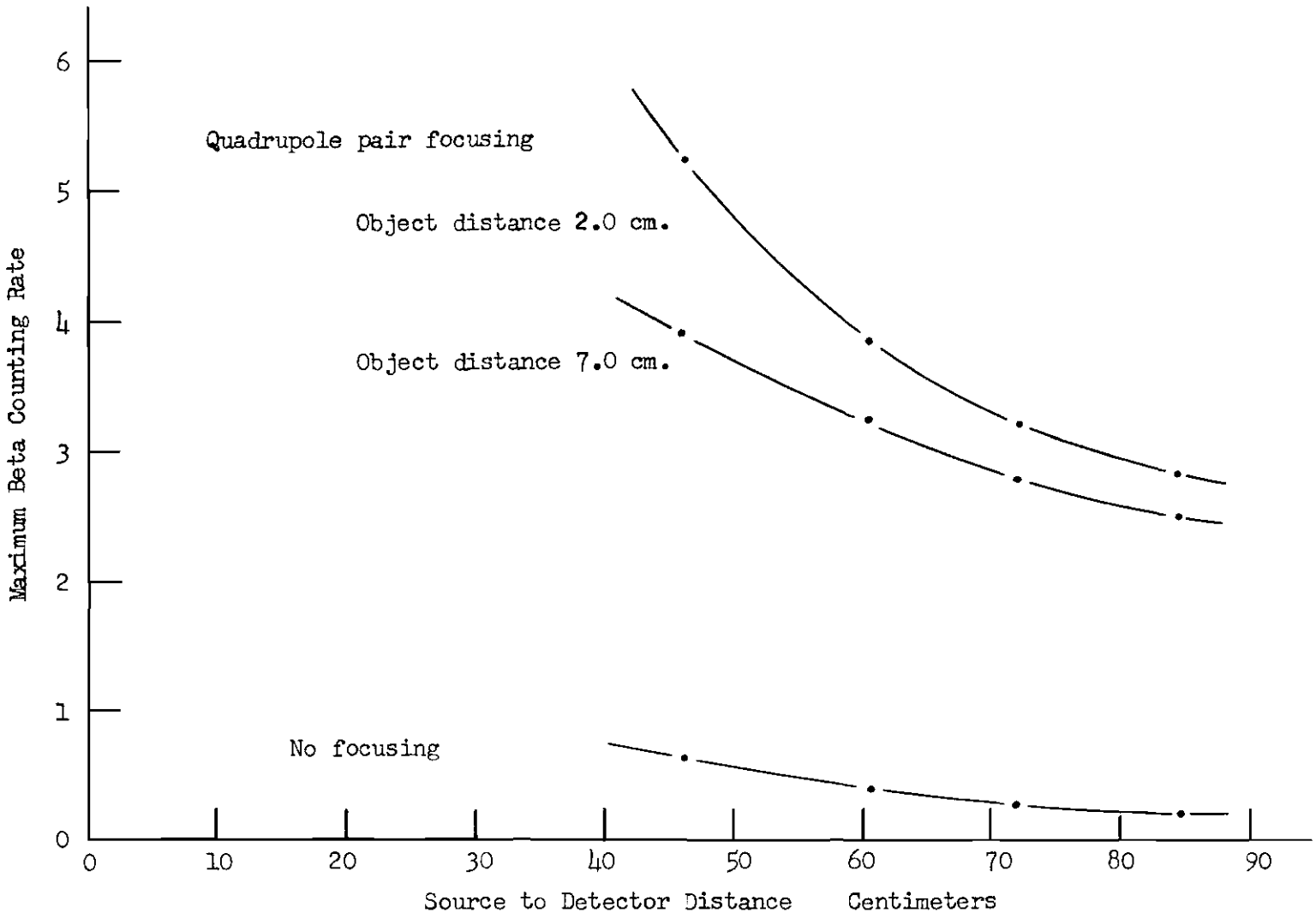

Figure 5. Maximum Beta Counting Rate versus Source-to-Detector Distance.

the lens. The effective solid angle subtended by the beta detector was determined by comparing the counting rate with that for a simple geometry. The effective source-to-detector distance for a 1.5 inch diameter scintillation crystal was found to be about 23 centimeters.

With the geometry of the electron focusing system fixed, a calibration plot of focusing currents in the two magnetic quadrupoles versus electron energy was obtained by maximizing the counting rate using the Cs^{137}, Sn^{113}, and Hg^{203} conversion electron sources. The energies of these conversion lines covered the range of beta energies observed in the 0.437 MeV beta group of Sb^{125}. This calibration plot is given in Figure 6. The error bars represent probable error in reading the ammeters. The plot for each focusing current was found to be linear through the three points. The focusing currents were such that the magnetic field at the pole faces was in the range of 80 to 200 gauss.

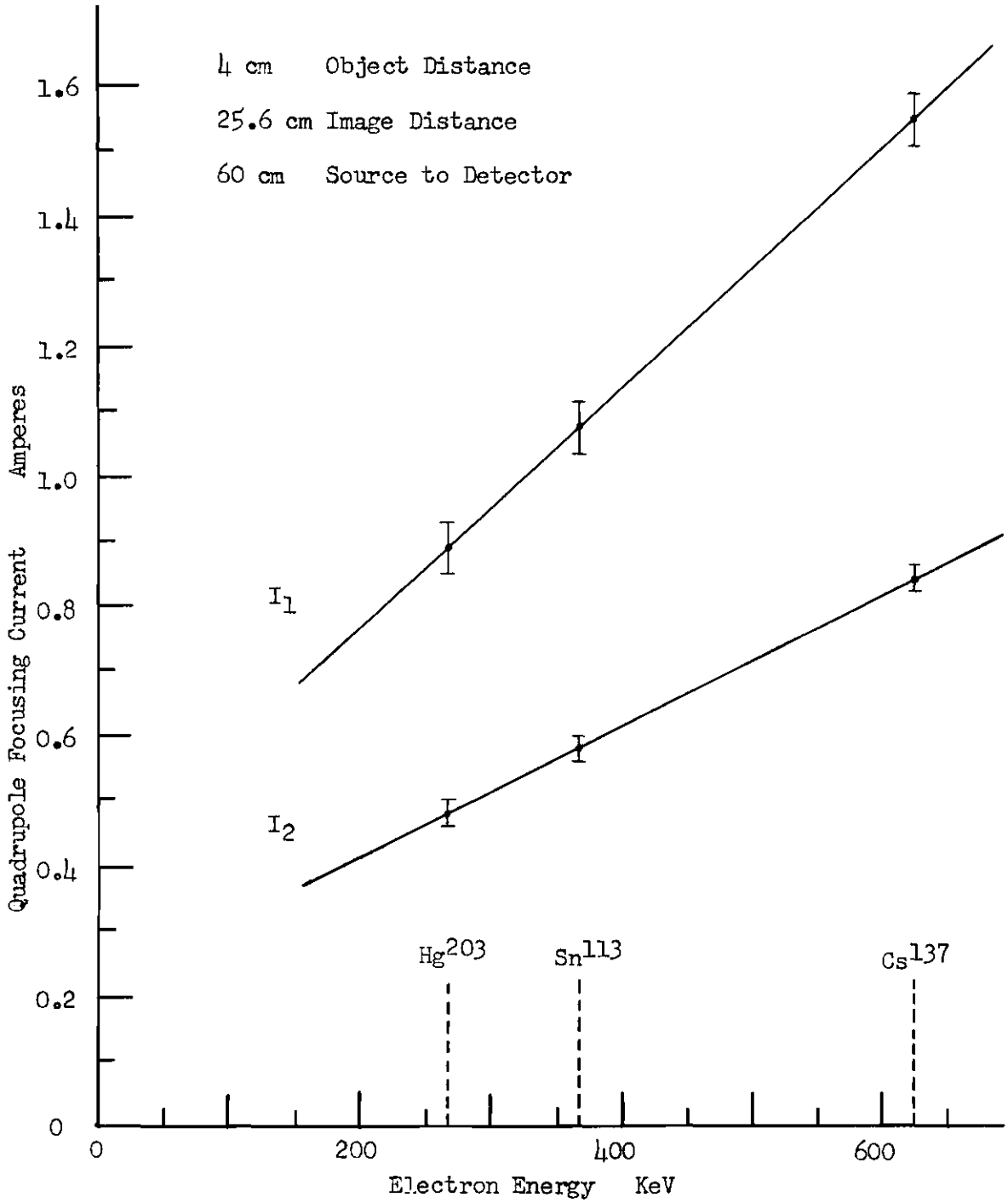

Figure 6. Electron Energy versus Quadrupole Focusing Currents.

CHAPTER IV

MEASUREMENT OF THE DIRECTIONAL CORRELATION

Sb^{125} was prepared at the Oak Ridge National Laboratory by means of the reaction Sn^{124} (n, γ) Sn^{125}. Sn^{125} decays by beta emission with ten day half-life into Sb^{125}. The Sb^{125} was obtained as a chloride in hydrochloric acid solution, and a source was prepared by the evaporation procedure discussed in Chapter III.

The gamma detector was necessarily positioned very close to the magnetic quadrupoles. A four-inch-long lucite light piper was inserted between the gamma scintillation crystal and the face of the photomultiplier tube to displace the photomultiplier tube from the highest magnetic field region. The tube was then magnetically shielded with a seven-inch-long cylinder of mu-metal. The gamma detector was also shielded with lead against gamma rays scattered off the iron in the focusing magnets. With the gamma pulse height analyzer set to accept the 0.176 MeV gamma line in Sb^{125} and the gamma detector unshielded, this scattered radiation was found to comprise about one-fourth of all gamma counts. Furthermore, the counting rate for scattered radiation was anisotropic. A two-millimeter-thick lead sheet was used to form a cylindrical shield around the NaI crystal and a conical shield around the geometrical solid angle subtended by the NaI crystal. These shields removed the anisotropy in the gamma counting rate due to detection of low energy scattered radiation.

The gamma spectrum of the Sb^{125} source, with the gamma detector shielded against scattered radiation, is given in Figure 7. This spectrum was obtained by scanning the energy range from zero to 0.700 MeV with a pulse height analyzer window width of about 0.010 MeV. This spectrum agrees closely with that obtained by Chandra and Pandharipande (24). Energy calibration was done with the 0.662 MeV gamma line of Cs^{137}, the 0.393 MeV gamma line of Sn^{113}, and the 0.279 MeV gamma line of Hg^{203}. The resolution of the 0.427 MeV gamma line in the Sb^{125} spectrum--defined as the full energy width of the line, at half maximum amplitude, divided by the energy of the line--was about 22 percent. The energy of gamma counts entering the slow coincidence circuit was selected by locating the center of a line on the gamma spectrum with a narrow pulse height analyzer window width and then widening the window about this center to accept most of the line.

Although the magnetic lens acted as a low resolution beta ray spectrometer, the energy of beta counts entering the slow coincidence circuit was selected by the pulse height analyzer. The magnet currents required to focus beta rays of a given energy were determined from the calibration plot, Figure 6. A pulse height analyzer window width of about 0.040 MeV was centered on the focused electron peak. This procedure resulted in the selection of beta rays of a given energy being independent of drifts in the electronic circuits.

The Sb^{125} source was centered with respect to the axis of rotation of the gamma detector by moving the axis of rotation to obtain less than 0.5 percent deviation in the gamma counting rate in the 90 degree, 180 degree, and 270 degree positions, with a narrow pulse height analyzer

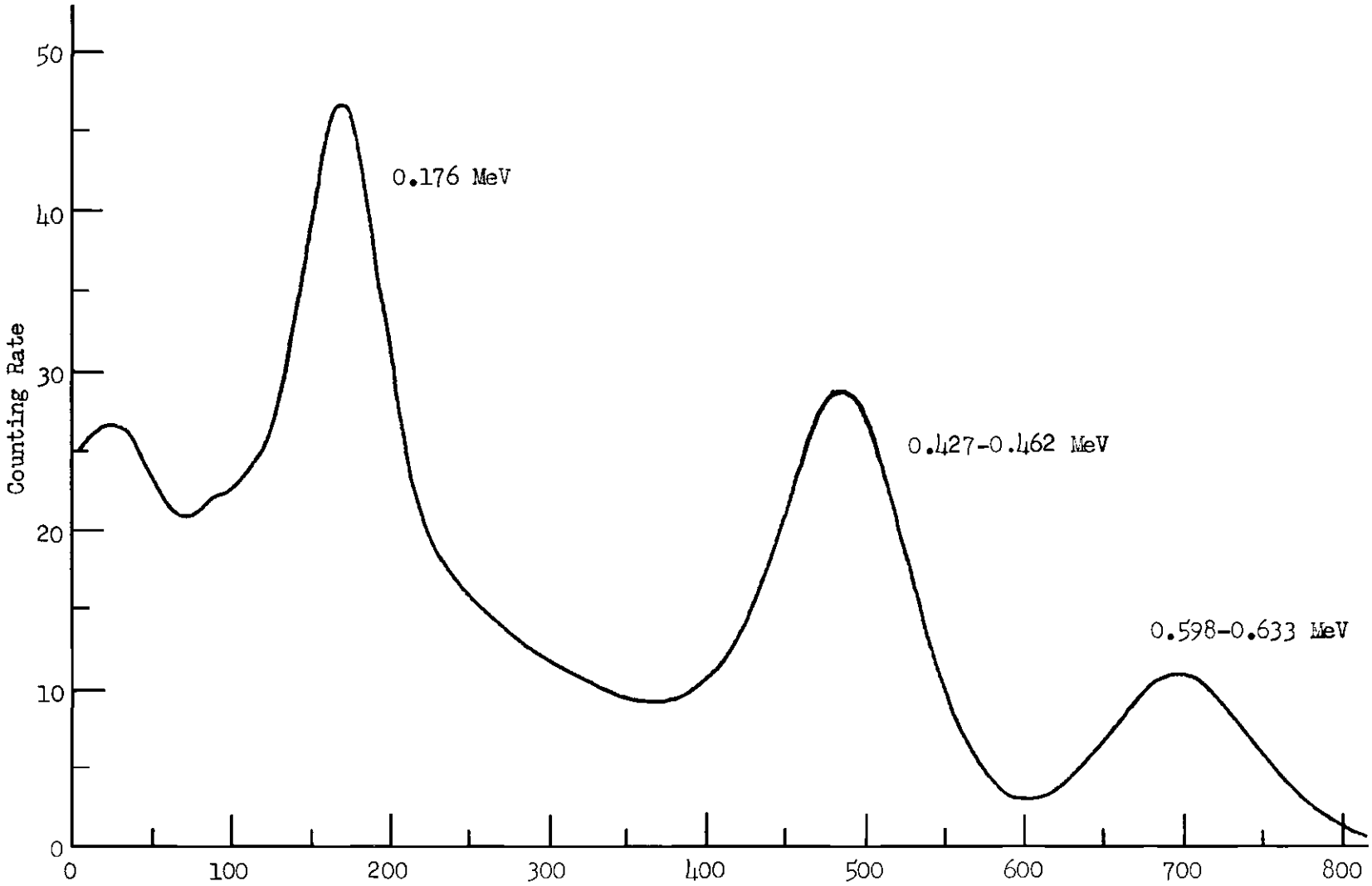

Figure 7. Sb^{125} Gamma Ray Spectrum.

window width centered on the 0.600 MeV gamma peak. In all experiments, the coincidence counting rates in the 90 degree and 270 degree positions were compared as a check of instrumental asymmetries. The directional correlation of the allowed 0.295 MeV beta group in Sb^{125} in coincidence with the 0.427 MeV gamma was measured as a final check of instrumental asymmetries. The results of this measurement are given in Table 1. The correlation was found to be isotropic. The gamma-gamma coincidence background was measured at beta pulse height analyzer settings over the range of beta energies. A 3/16 inch thick lucite disc was inserted in the source end of the vacuum chamber to absorb all beta rays, and the focusing magnets were demagnetized to avoid focusing any secondary electrons produced in the lucite. The average ratio of the real plus accidental gamma-gamma coincidence counting rate to the real beta-gamma coincidence counting rate was less than 0.3 percent for every experiment. Therefore, the gamma-gamma coincidence background was considered negligible.

The directional correlation of the 0.437 MeV beta group in Sb^{125} in cascade with the 0.176 MeV gamma was measured at four beta energies between 0.250 MeV and 0.410 MeV. This energy range was limited at the low end by the presence of another beta group in coincidence with the 0.176 MeV gamma. The accidental coincidence rate was measured periodically by inserting a 0.4 microsecond time delay in the beta channel. This accidental counting rate was checked by removing and shielding the gamma detector from the Sb^{125} source and then introducing another source to the gamma detector so as to reproduce the original gamma counting rate. The reduction of experimental data to obtain the A_2 coefficient is outlined in Appendix C. The correction for the geometrical solid angle sub-

tended by the detectors is discussed in Appendix D. The results of the directional correlation measurements are tabulated in Table 2 and graphed in Figure 8. This graph shows individually the results of nine different experiments performed over a period of seven months to demonstrate the reproducibility of results. The error bars represent probable statistical errors. The A_2 coefficient for the directional correlation increases rapidly and monotonically with energy. The disagreement at the highest energy is probably statistical in nature. The low beta counting rate near the beta end-point energy necessitated a counting time of several weeks.

The gamma spectrum in coincidence with the 0.437 MeV beta group was measured with the beta pulse height analyzer set to accept beta rays in the energy range 0.315 - 0.390 MeV. This spectrum is given in Figure 9. The gamma spectrum in coincidence with the 0.437 and 0.295 MeV beta groups was measured with the beta pulse height analyzer set to accept beta rays in the energy range 0.235 - 0.275 MeV. This spectrum is given in Figure 10. Both spectra agree with the Sb^{125} decay scheme given in Figure 1. The beta energy range 0.235 - 0.275 MeV was that used to make the lowest beta energy measurement of the A_2 coefficient. Figure 10 suggests that some gamma counts corresponding to an energy of 0.176 MeV in the Compton distribution from the 0.427 and 0.462 MeV gamma transitions were observed in coincidence with beta counts in the energy range 0.235 - 0.275 MeV from the allowed 0.295 MeV beta transition. It was estimated that these coincidences could possibly contribute up to eight percent of the area under the coincidence spectrum peak at gamma energy 0.176 MeV. These coincidences from an allowed beta transition would have an isotropic directional correlation with the result that the lowest beta energy measurement of the A_2 coefficient could be too small by as much as 12 percent.

Table 1. Sb^{125} Directional Correlation Data for the 0.295 MeV Beta Group and the 0.427 MeV Gamma

Beta energy range, MeV	Total real coincidences 180 degrees	Ratio of real to accidental counting rates	Total accid. coincidences	Anisotropy	Probable statistical error
0.235 - 0.275	16,000	3	2,700	-0.002	0.012

Table 2. Sb^{125} Directional Correlation Data for the 0.437 MeV Beta Group and the 0.176 MeV Gamma

Beta energy range, MeV	Total real coincidences 180 degrees	Ratio of real to accidental counting rates	Total accid. coincidences	Anisotropy	A_2 (uncorrected)	A_2 (corrected)	Probable statistical error
0.285 - 0.325	14,100	6	1,000	0.210	0.131	0.140	0.007
0.235 - 0.275	28,200	5.5	3,900	0.128	0.082	0.088	0.005
0.335 - 0.375	21,800	5	2,500	0.278	0.170	0.182	0.005
0.385 - 0.425	13,300	2	7,400	0.369	0.219	0.235	0.008
0.235 - 0.275	13,700	5.5	1,300	0.160	0.101	0.109	0.007
0.385 - 0.425	14,500	2	10,100	0.290	0.176	0.189	0.007
0.235 - 0.275	34,300	5.5	3,800	0.156	0.099	0.106	0.004
0.335 - 0.375	21,400	5	2,900	0.290	0.176	0.189	0.005
0.285 - 0.325	19,600	6	2,600	0.187	0.117	0.126	0.005

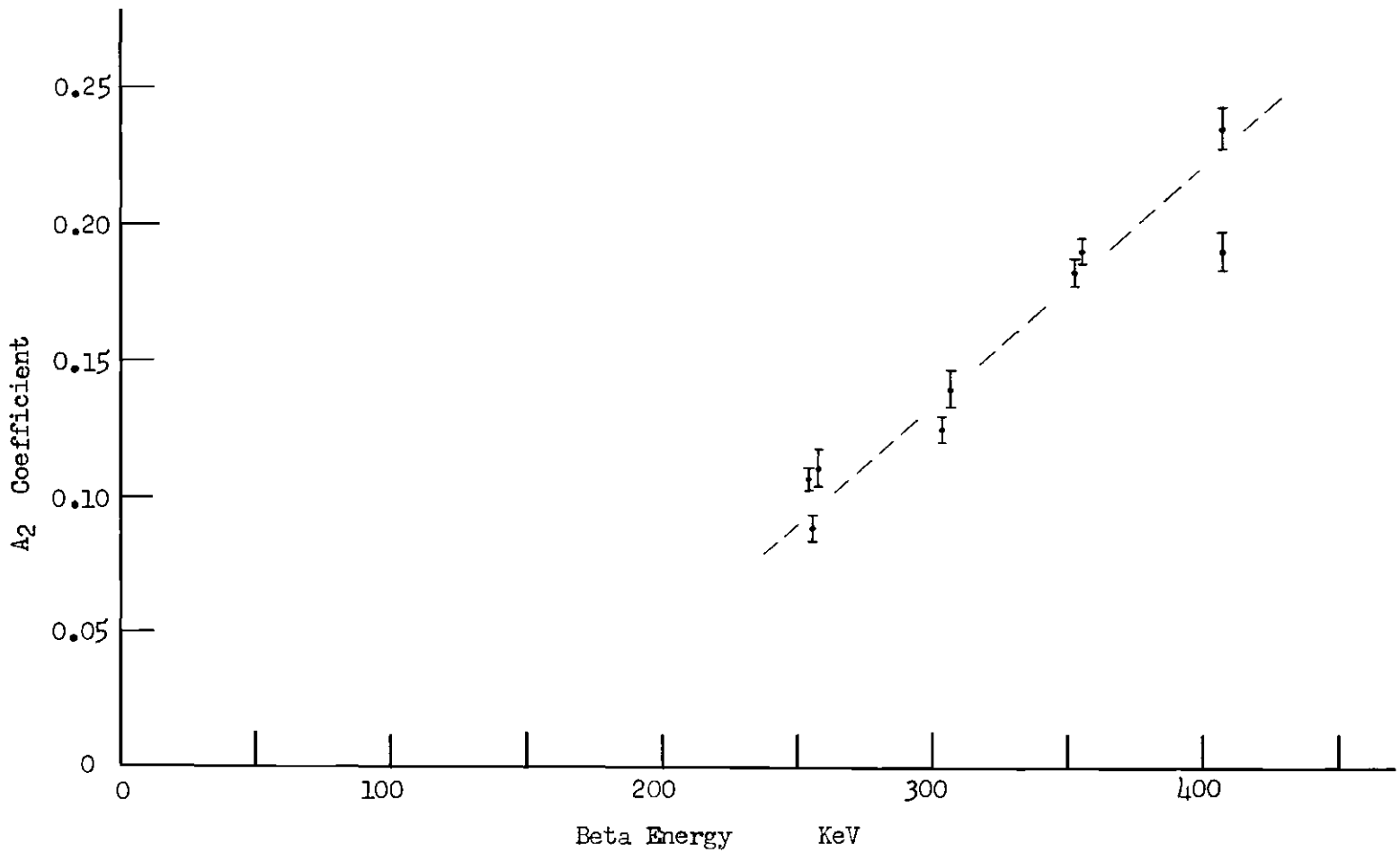

Figure 8. Experimental Directional Correlation A_2 Coefficient.

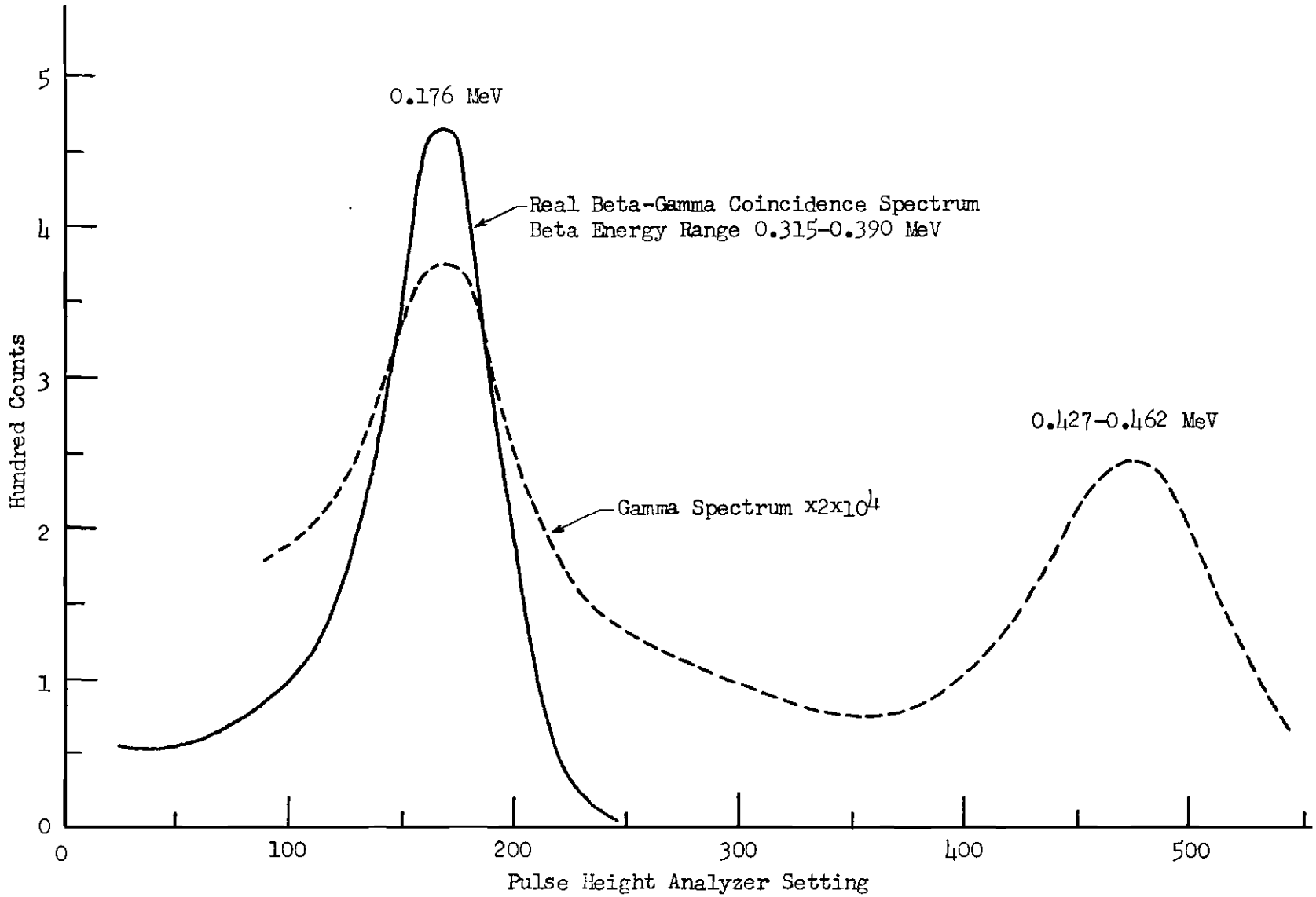

Figure 9. Gamma Coincidence Spectrum with the 0.437 MeV Beta Group.

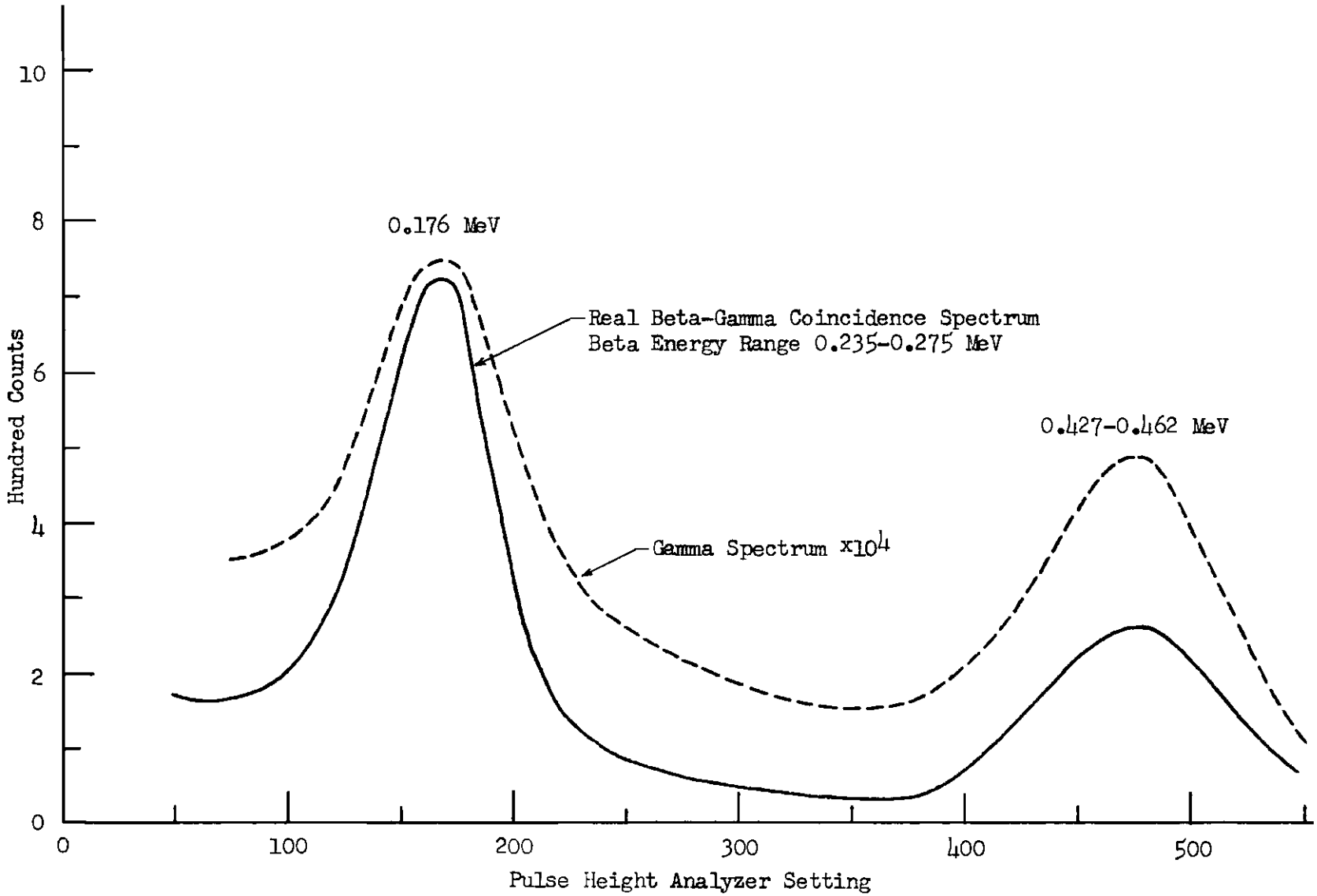

Figure 10. Gamma Coincidence Spectrum with the 0.437 and 0.295 MeV Beta Groups.

CHAPTER V

ANALYSIS OF THE BETA TRANSITION

Analysis of the Intermediate State Spin

The 0.437 MeV beta transition in the decay of Sb^{125} involves a spin change of two units if the spin of the 0.321 MeV excited state in Te^{125} is 11/2. In this case, the only operative nuclear matrix element of the beta decay interaction Hamiltonian is the B_{ij} matrix element; the beta transition is said to be unique. The A_2 coefficient may be factored into two parts, one dependent on the beta transition and the other dependent on the gamma transition (see Appendix B). The beta factor may be calculated without ambiguity for this case. The gamma factor may be normalized out by arbitrarily matching experimental and theoretical values for the A_2 coefficient at one beta energy. This matching may be achieved by adjusting the unknown gamma multipole mixing ratio.

Figure 11 gives a graph of the theoretical A_2 coefficient versus beta energy, assuming the intermediate state spin is 11/2, calculated from the formulas of Kotani (13). The formulas of Morita and Morita (17), using the electron functions of Bhalla and Rose (15), gave results negligibly different from these. The theoretical A_2 coefficient was adjusted arbitrarily to the experimental value, $A_2 = 0.140$, at beta energy 0.305 MeV. The experimental A_2 coefficients are also plotted. The different experimental values at a given beta energy were averaged, each value being

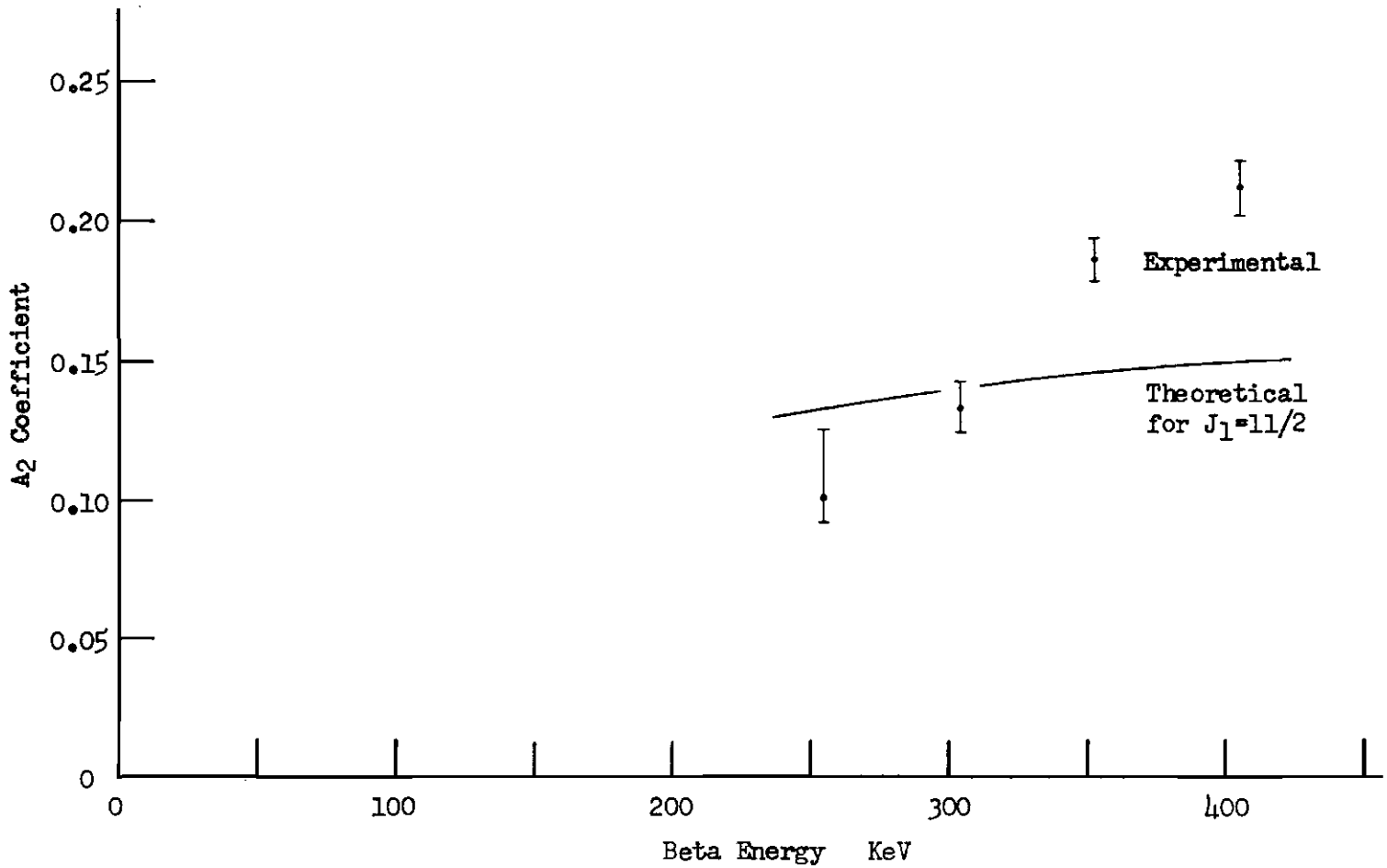

Figure 11. Theoretical Directional Correlation A_2 Coefficient for $J_1=11/2$.

weighted by the total number of real coincidence counts in the 180 degree counting position. The error bar for the lowest beta energy measurement is extended to show the possible magnitude of the correction discussed at the end of Chapter IV. The experimental and theoretical A_2 coefficients are seen to have much different dependence on the beta energy. This disagreement indicates that the spin of the 0.321 MeV excited state in Te^{125} is not 11/2.

If the intermediate state spin is 7/2, the 0.437 MeV beta transition involves no spin change, and all six nuclear matrix elements listed in Table 3 may be operative. A meaningful analysis of the beta transition is rendered impossible by the presence of five independent, unknown, nuclear matrix element ratios. It will be assumed, in accord with Narcisi (25) and the evaluation of the Nuclear Data Group (26), that the 0.176 MeV gamma transition indeed involves some M1 radiation, thereby eliminating the possibility of spin assignment 7/2. Then the 0.321 MeV excited state in Te^{125} must be a 9/2- state.

Nuclear Model Predictions

The Te^{125} nucleus contains 52 protons and 73 neutrons. The shell model (18) for a single odd neutron predicts the three lowest states in Te^{125} having spins and parities 1/2+, 3/2+, and 11/2-. However, this model does not predict a 9/2- state. Glendenning has calculated the low-lying even-parity states in Te^{125} from the intermediate coupling model (35). The odd neutron is assumed to have available single particle states $3s_{1/2}$ and $2d_{3/2}$ and to be weakly coupled to collective surface vibrations of the nuclear core. This theory predicts the 1/2+ and 3/2+ states. No state is

predicted around 0.321 MeV. It is inferred, therefore, that the 0.321 MeV state in Te^{125} is an odd-parity state. Rassey has calculated the energy states of a single neutron in the field of a strongly deformed nuclear core (36). These calculations differ from those of Mottelson and Nilsson (37) in that Rassey used the eigenvectors of a three-dimensional anisotropic (rather than isotropic) harmonic oscillator as basis vectors. Narcisi extrapolated Rassey's results to a deformation parameter of 0.06, determined from the electric quadrupole moment of Te^{125}, and found that this theory predicts odd-parity levels of spin 7/2, 9/2, and 11/2 (25). No one of the common nuclear models gives a full description of the low-lying excited states in Te^{125}.

Analysis of the Nuclear Matrix Elements

The theoretical treatment of the beta-gamma directional correlation is outlined in Appendix B for a beta transition involving one unit of nuclear spin change. The formulas contain three independent nuclear matrix element parameters Υ, x, and u, and the gamma multipole mixing ratio δ, defined in Appendix B. The ratio of the directional correlation A_2 coefficients at two different beta energies is independent of the mixing ratio δ. If the ratio $A_2(W_1)/A_2(W_2)$ and the parameters Υ and x are treated as independent variables, one obtains a fourth-order equation in parameter u which may be solved algebraically. If the A_2 coefficient at one beta energy and the three parameters Υ, x, and u are treated as independent variables, one obtains a quadratic equation in the mixing ratio δ.

No a priori knowledge of the parameters x and u exists. Using the single particle model of an odd mass number nucleus having uniform particle

density, Ahrens and Feenberg (38) have calculated an estimate of the parameter Υ given by the expression

$$\Upsilon = 1 + (W_o - 2.5)\frac{A^{1/3}}{Z}.$$

Here A and Z are the mass number and atomic number, respectively, of the nucleus, and W_o is the beta transition total end-point energy in units of electron rest energy mc^2. Fujita (43) and Eichler (44) have obtained estimates for Υ based on the conserved vector current theory of the beta decay interaction. Their conclusions may be represented as

$$\Upsilon = 2.4 + (W_o - 2.5)\frac{A^{1/3}}{Z}.$$

For the 0.437 MeV beta transition in Sb^{125},

$$(W_o - 2.5)\frac{A^{1/3}}{Z} = -0.06.$$

The solution for the fourth-order equation in parameter u was programmed for the Burroughs B5500 computer at the Rich Electronic Computer Center using the formulas of both Kotani (13) and Morita and Morita (17) for the A_2 coefficient. The ratio of the A_2 coefficients at beta energies 0.368 MeV and 0.287 MeV, corresponding to normalized beta momenta of 1.4 and 1.2, respectively, was taken from a straight line drawn between these energies to best fit the experimental points of Figure 11. A greater

ratio and a lesser ratio, determined by consideration of the experimental error limits, were also used in separate computer calculations. The parameter Υ was varied from zero to five in steps of one-half and the parameter x was varied from minus ten to plus ten in steps of unity. Interesting regions of the $x\Upsilon$ plane determined from these calculations were subsequently investigated with a finer grid for the independent variables x and Υ. For each solution for parameter u, the quadratic equation in the mixing ratio δ was solved using an experimental value for the A_2 coefficient at beta energy 0.287 MeV.

Results of the computer calculations are graphed in the three parts of Figure 12. All combinations of x and Υ which were investigated gave two real solutions for u. Only one solution for u, at most, gave real solutions for the mixing ratio. The three parts of Figure 12 show regions of the $x\Upsilon$ plane in which real solutions for the mixing ratio were obtained. The graphs represent solutions obtained using the formulas of Morita and Morita (17) and the electron functions of Bhalla and Rose (15). The behavior of parameter u is indicated by the slope of the cross-hatching as specified in the key of each graph. Region C contains negative values of both u and δ; Regions A and B contain positive values of both u and δ. Solutions for parameter u using the formulas of Kotani (13) gave regions in the $x\Upsilon$ plane having real solutions for the mixing ratio very similar in appearance to those graphed in Figure 12. In general, Region B is displaced upward in the Υ direction by about 0.4, and Region C is wider and extends to larger negative values of x. Both parameters x and u are bounded away from zero; so the nuclear matrix elements $\int \bar{\sigma} \times \bar{r}$ and $\int \bar{r}$ make an appreciable contribution to the beta decay transition. The para-

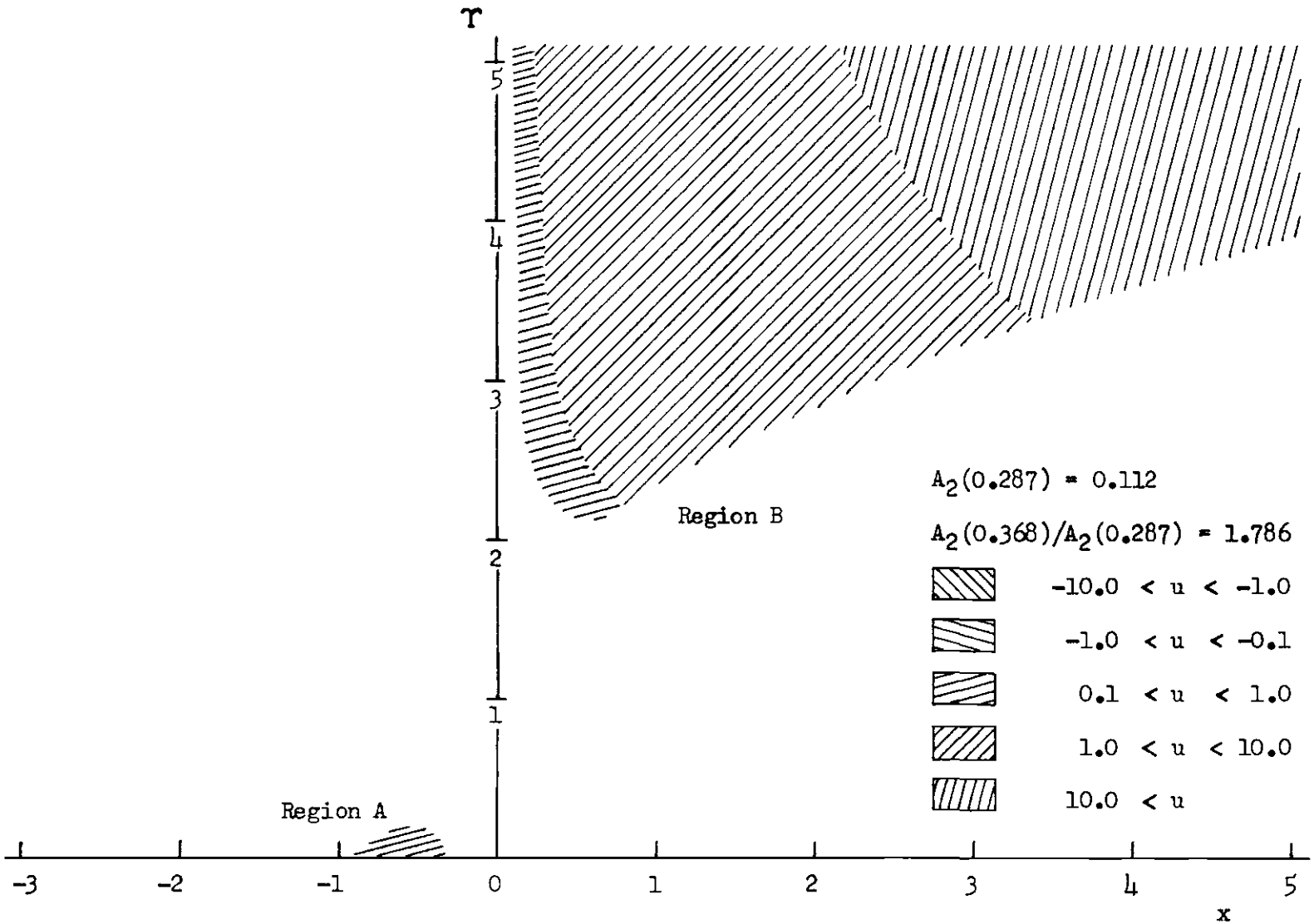

Figure 12a. Nuclear Matrix Element Parameters Consistent with the Experimental A_2 Coefficient.

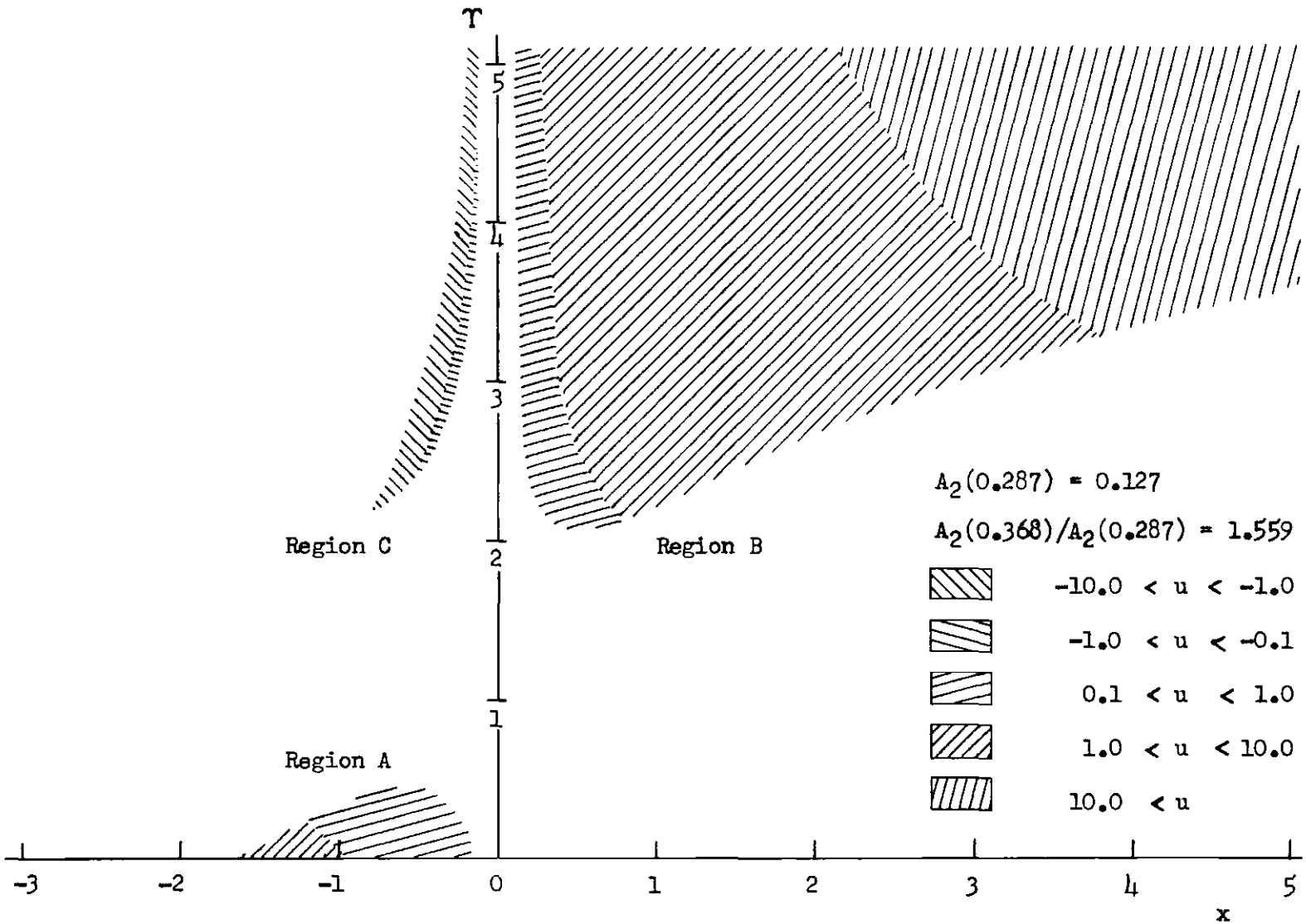

Figure 12b. Nuclear Matrix Element Parameters Consistent with the Experimental A_2 Coefficient.

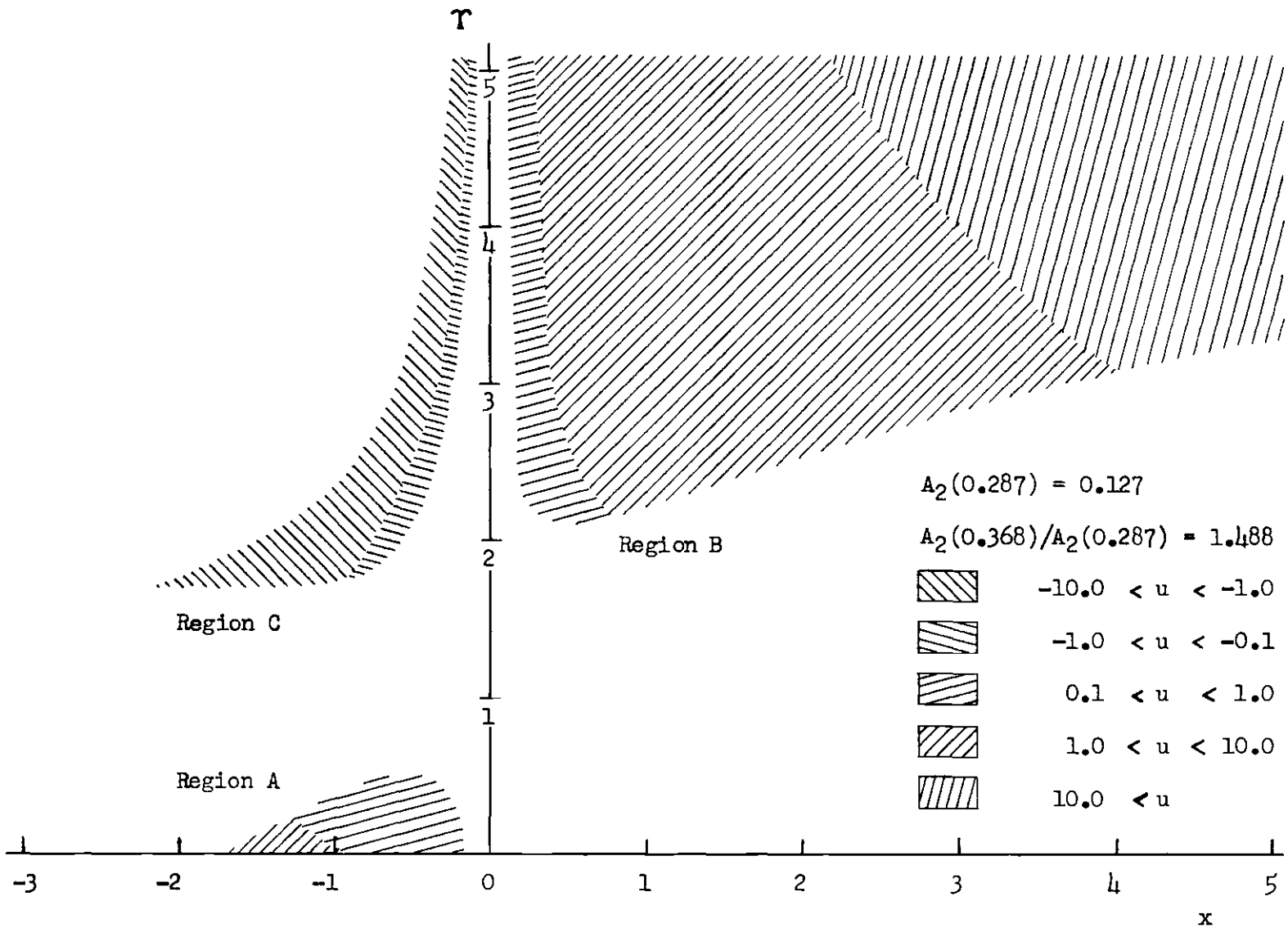

Figure 12c. Nuclear Matrix Element Parameters Consistent with the Experimental A_2 Coefficient.

meter Υ is seen to have a forbidden range extending from about 0.6 to 1.6. Possible solutions for Υ exist which are compatible with the approximate value predicted by Fujita (43) but not with that predicted by Ahrens and Feenberg (38).

The pair of solutions to the quadratic equation in the mixing ratio δ consisted in general of one solution representing a predominantly M1 gamma transition and the other solution representing a predominantly E2 gamma transition. A predominantly M1 transition would be expected on the basis of the single particle model. A predominantly E2 transition would indicate strong collective nuclear motion.

The beta energy dependence of the A_2 coefficient was calculated in a second computer program using about one hundred sets of independent variables Υ, x, u, and δ, corresponding to points over the entire range of solutions in the graphs of Figure 12. No significant difference in the energy dependence of the A_2 coefficient was found among these various sets of variables. A few representative curves of these calculations of the A_2 coefficient versus beta energy are given in Figure 13, superimposed upon the experimental data points.

The second computer program also calculated the ratio of the beta energy spectrum shape correction factors at beta energies 0.410 MeV and 0.287 MeV. These results are represented by contour lines in the xΥ plane of Figure 14. The corresponding shape factor ratio for a unique beta transition is 1.48. It appears that an accurate measurement of this shape factor ratio could decide for or against Region A which involves a range of parameter Υ smaller than that predicted by any theory.

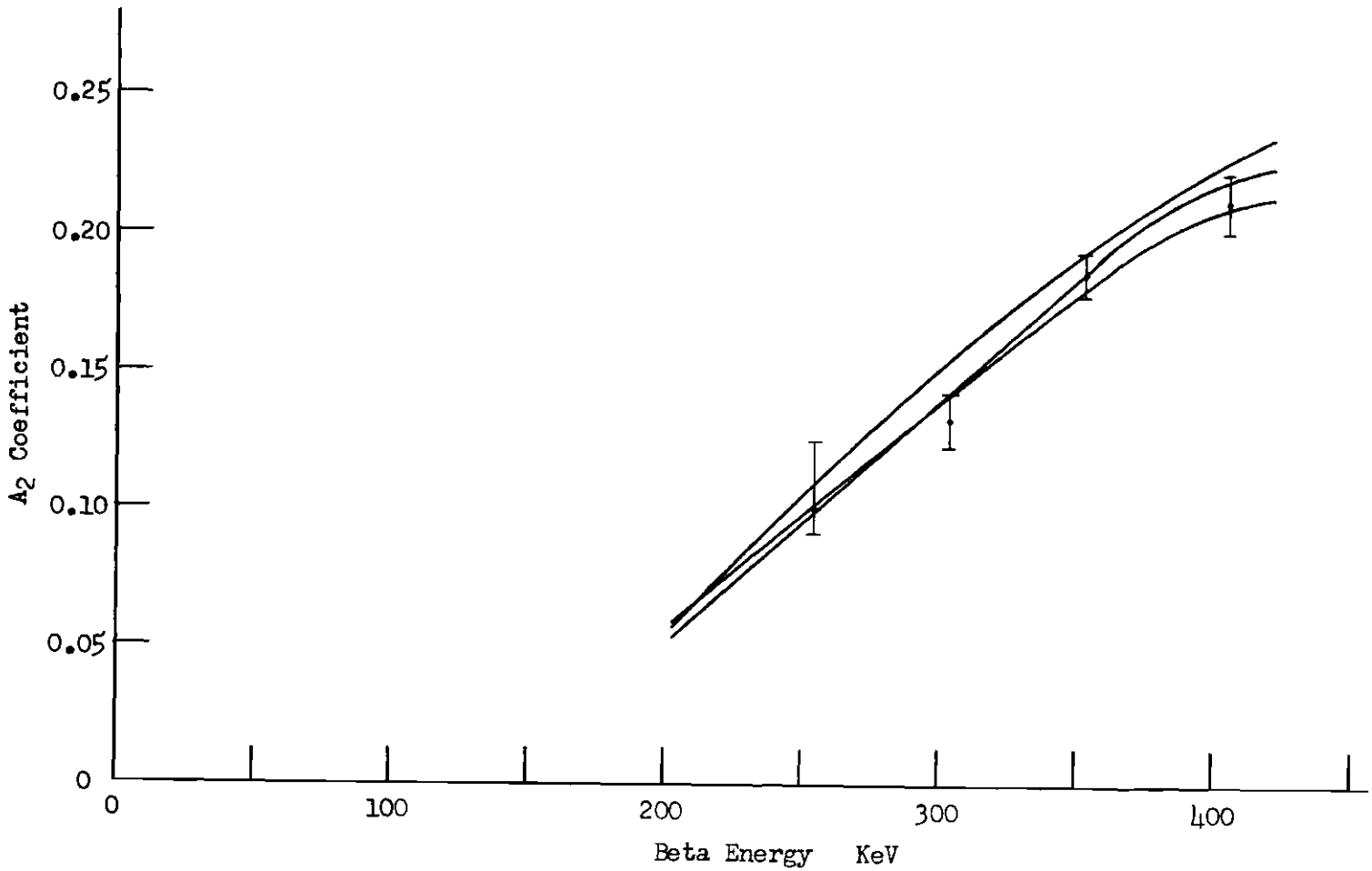

Figure 13. Theoretical Directional Correlation A_2 Coefficient for $J_1 = 9/2$.

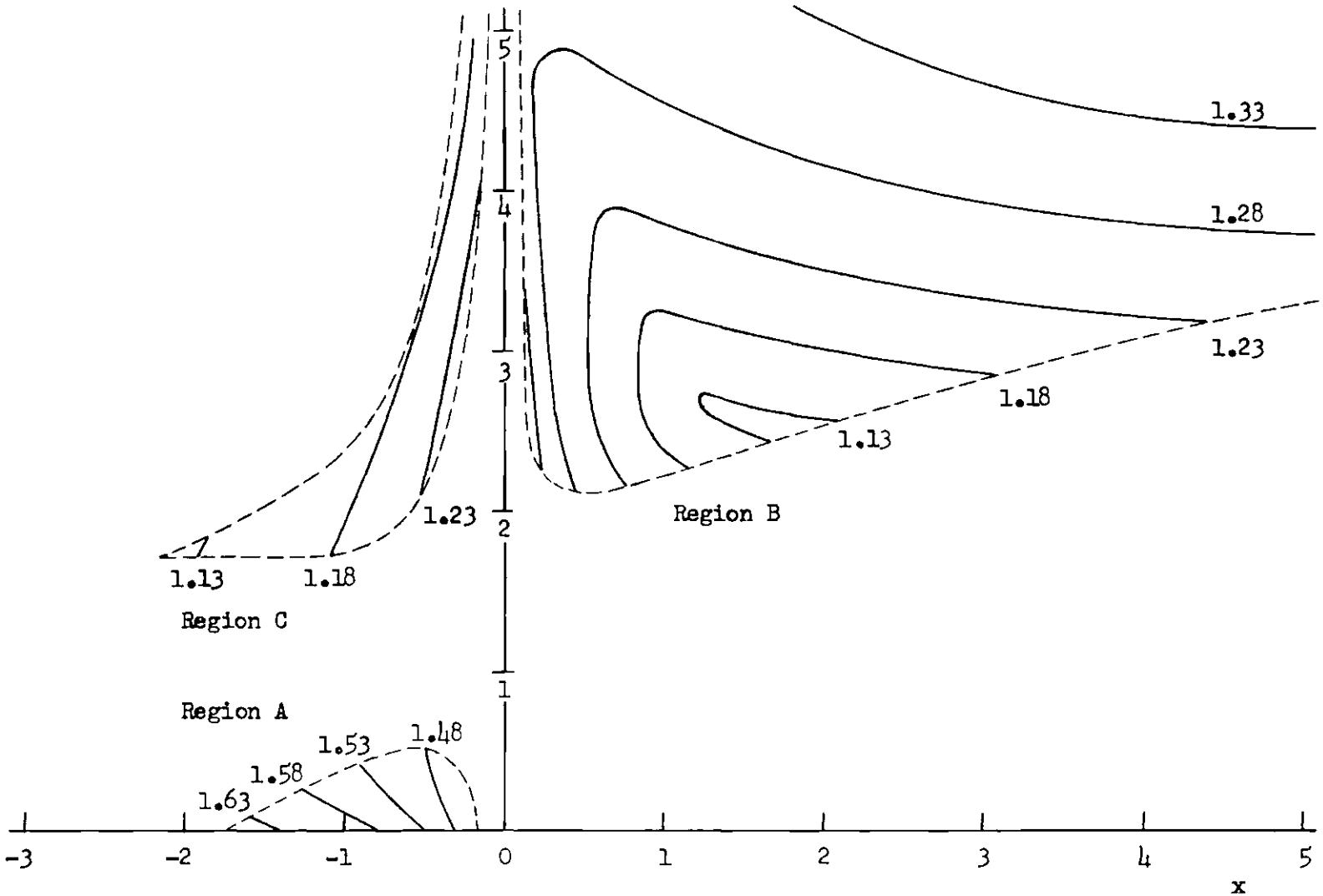

Figure 14. Ratio of the Shape Correction Factors at Beta Energies 0.410 MeV and 0.287 MeV.

CHAPTER VI

RECOMMENDATIONS FOR FUTURE RESEARCH

Much information about the excited energy states of Te^{125} which are populated by the beta decay of Sb^{125} remains to be established. Narcisi alone has attempted a systematic investigation of the spin and parity of the Te^{125} states above 0.462 MeV. Furthermore, conclusive elimination of the possibility of a spin assignment of 7/2 for the 0.321 MeV state requires more reliable information about the multipole mixing of the 0.176 MeV gamma ray. Determination of this mixing ratio by a gamma-gamma angular correlation would be difficult because of the complicated decay scheme of Sb^{125} and the unknown nature of the other gamma rays in coincidence with the 0.176 MeV gamma ray. Measurement of the ratio of the conversion coefficients for the L_{II} and L_{III} subshells would permit an accurate determination of this mixing ratio with the subsequent possibility of more severe limitations on the relative magnitudes of the nuclear matrix elements operative in the 0.437 MeV beta transition.

The magnetic quadrupole lens used to focus beta rays in this experiment is useful for any beta-gamma angular correlation study where a gamma-gamma coincidence background tends to obscure the true correlation. The electronic circuits used in this experiment are sufficiently stable that real coincidence counting rates of only a few counts per minute are tolerable. Two modifications of the equipment are suggested for future applications:

1. The energy resolution could be greatly improved by using solid-state detectors. This would make it possible to select from complicated decay schemes more beta-gamma and conversion electron-gamma coincidences for the purpose of determining nuclear spins and parities, gamma multipole orders, and the relative magnitudes of nuclear matrix elements of the beta decay interaction Hamiltonian.

2. Additional gamma detectors, with their associated electronics, could be positioned about the radioactive source to measure coincidence rates simultaneously at all angles necessary to determine an angular correlation. This would make it possible to study short-lived nuclides created by neutron capture.

APPENDICES

APPENDIX A

FOCAL LENGTHS AND PRINCIPAL PLANES OF A MAGNETIC QUADRUPOLE

APPENDIX A

FOCAL LENGTHS AND PRINCIPAL PLANES OF A MAGNETIC QUADRUPOLE

The analysis of focusing parameters is adapted from Weidemann (32). Reference is made to Figure 15 illustrating the focusing geometry.

Consider an electron incident along a line parallel to the z axis through the center of the quadrupole. The force on the electron is given by

$$-e\bar{v} \times \bar{B} = \frac{d\bar{p}}{dt} = mg \frac{d\bar{v}}{dt} ,$$

where $\bar{v}$ and $\bar{p}$ are the velocity and momentum, respectively, of an electron of mass m and charge -e, $\bar{B}$ is the magnetic field, and

$$g = \left(1 - \frac{v^2}{c^2}\right)^{-\frac{1}{2}} .$$

Motion in the Divergent xz Plane

$$-e(-v_z B_y) = mg \frac{dv_x}{dt} .$$

$$B_y(x) = B_y(0) + x \left.\frac{\partial B_y}{\partial x}\right|_o , \text{ where } B_y(0) = B_x(0) = 0 .$$

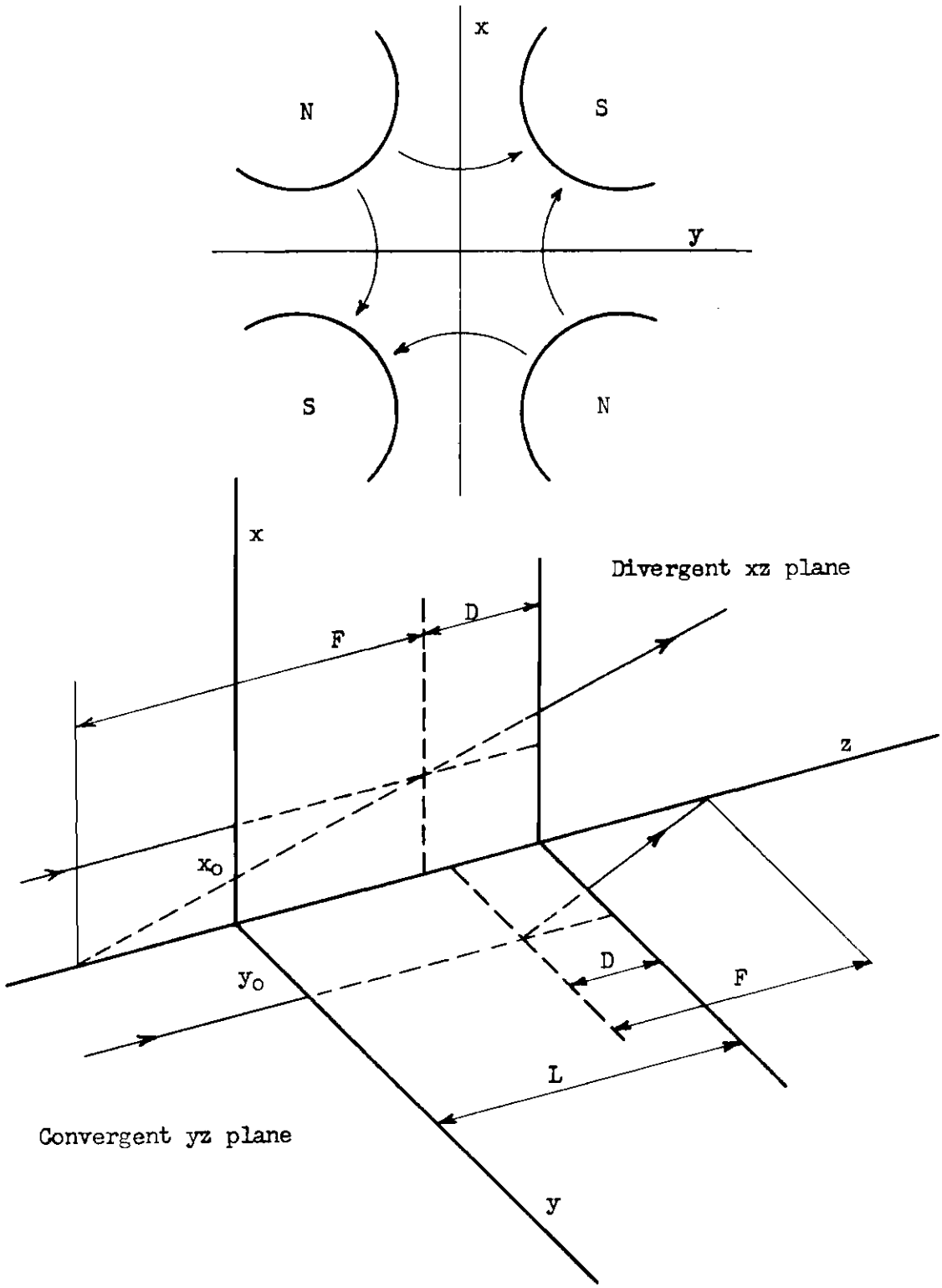

Figure 15. Electron Trajectories in a Magnetic Quadrupole.

A necessary focusing condition is that $\frac{\partial B_y}{\partial x} = \frac{\partial B_x}{\partial y}$ = a constant at every point in the magnetic field. This focusing condition requires that the shape of the magnetic pole faces be a hyperbola of infinite extent; but it is approximated in the region about the z axis by a circular shape.

$$\frac{d^2x}{dt^2} = v_z^2 \quad \frac{d^2x}{dz^2} = \frac{ev_z}{mg} \times \frac{\partial B_y}{\partial x} .$$

$$\frac{d^2x}{dz^2} - K^2x = 0 , \qquad \text{where } K^2 = \frac{e}{mv_z g} \frac{\partial B_y}{\partial x} .$$

The following boundary conditions are imposed upon the solution:

$$\left.\frac{\partial x}{\partial z}\right|_{z=o} = 0$$

$$x|_{z=o} = x_o .$$

Then $x = x_o \cosh Kz$.

The focal length F and the location of the principal plane relative to the face of the lens are obtained from the relation

$$\left.\frac{\partial x}{\partial z}\right|_{z=L} = Kx_o \sinh KL = \frac{x_o}{F} = \frac{x_o \cosh KL - x_o}{D} .$$

$$\frac{1}{F} = K \sinh KL$$

$$\frac{1}{D} = \frac{K \sinh KL}{\cosh KL - 1}$$

The object distance P and the image distance Q are related through the lens formula $\frac{1}{P} + \frac{1}{Q} = \frac{1}{F}$, and the magnification is the ratio of image distance to object distance.

Motion in the Convergent yz Plane

$$-e(v_z B_x) = mg \frac{dv_y}{dt} .$$

$$y = y_o \cos Kz$$

$$\frac{1}{F} = K \sin KL$$

$$\frac{1}{D} = \frac{K \sin KL}{1 - \cos KL}$$

APPENDIX B

OUTLINE OF THE THEORETICAL FORMALISM

APPENDIX B

OUTLINE OF THE THEORETICAL FORMALISM

The outline of the theory is adapted from Preston (11), Kotani (13), and Morita and Morita (17).

The Beta Decay Transition

The Sb^{125} beta decay transition involves the transformation of a neutron inside the atomic nucleus into a proton with the simultaneous emission of a negative electron and an anti-neutrino. Since the beta decay interaction is weak compared to electromagnetic and nucleon-nucleon interactions, this transformation may be treated by the techniques of first-order time-dependent perturbation theory. The beta decay transition probability per unit time is given by

$$\frac{4\pi^2}{h}|(f|H|i)|^2 \rho(E) ,$$

where $\rho(E)$ is the phase space density of final quantum states available to the electron and neutrino, and $(f|H|i)$ is the matrix element of the beta decay interaction Hamiltonian between state vectors representing the initial and final states of the physical system. The number of transitions per unit time with electron momentum between p and p + dp is given by

$$N(p)\ dp = \frac{4\pi^2}{h}|(f|H|i)|^2 \left(\frac{4\pi}{h^3}\right)^2 \frac{(E_o - E)^2}{c^3} p^2\ dp .$$

E is the total electron energy, and E_o is the total energy difference between initial and final nuclear states. It is customary to express electron energy in terms of mc^2 and electron momentum in terms of mc. We make the substitutions $W = \frac{E}{mc^2}$ and $P = \frac{p}{mc}$ such that $W^2 = P^2 + 1$. Furthermore, the energy distribution, $N(W)dW$, must be multiplied by the Fermi function $F(Z, W)$ which corrects for the effect of the nuclear Coulomb force acting on the emitted electron.

$$N(W)\ dW = 2\pi |(f|H|i)|^2 \frac{1}{4\pi^4} (W_o - W)^2\ P\ W\ F(Z,W)\ dW.$$

Non-conservation of parity in the beta decay interaction implies that the matrix element of the beta decay interaction Hamiltonian may be either a scalar or a pseudoscalar quantity. Invariance of the matrix element under a Lorentz transformation of coordinates implies that the matrix element may be formed as the inner product of a nuclear matrix element and a lepton matrix element of the same tensor rank identified by their transformation properties as either scalar, pseudoscalar, vector, pseudovector, or second-rank tensor quantities. The formulation of the matrix element is discussed in detail by Preston (11). The nuclear matrix element is limited experimentally to be either a vector or a pseudovector quantity. The different terms of the nuclear matrix element impose different selection rules on the change in angular momentum and parity between the initial and final nuclear states. A given beta decay transition is classified according to the selection rules imposed by the nuclear matrix elements which are operative for that transition. The allowed and

first-forbidden classifications are given in Table 3 along with the symbolic representation of the nuclear matrix elements which give the main contribution.

Table 3. Beta Decay Transitions

Transition Classification	Selection Rules	Nuclear Matrix Elements
Allowed	$\Delta J = 0, \pm 1$	$\int 1 , \int \overline{\sigma}$
	$\pi_i/\pi_f = +1$	
First-forbidden	$\Delta J = 0, \pm 1, \pm 2$	$\int \overline{\sigma}\cdot\overline{r} , \int \gamma_5 ,$
	$\pi_i/\pi_f = -1$	$\int \overline{\sigma} \times \overline{r} , \int \overline{\alpha} , \int \overline{r},$
		$\int B_{ij}$

The energy spectrum of the emitted electron is analyzed through the relationship

$$\left(\frac{N(W)}{P\ W\ F(Z,W)} \right)^{\frac{1}{2}} = \text{const}\ (W_o - W)\ C(W)^{\frac{1}{2}} .$$

A plot of the left-hand-side versus electron energy W is called a Fermi plot. C(W) is the shape correction factor required to make the plot a straight line. The intercept of this line with the abscissa gives the beta decay end-point energy W_o. For allowed transitions, the matrix ele-

ment of the beta decay interaction Hamiltonian is strictly independent of electron energy and C(W) is unity. A forbidden transition for which C(W) is actually independent of W is said to have an allowed shape.

The decay constant for the beta decay transition is given by

$$\lambda = \frac{\ln 2}{t} = \int_1^{W_o} N(W)\, dW,$$

where t is the half-life of the transition. The quantity $\log_{10} ft$ is taken as an index of the magnitude of the nuclear matrix elements that govern the transition, where f is defined as

$$f = \int_1^{W_o} (W_o - W)^2\, P\, W\, F(Z,W)\, C(W)\, dW\ .$$

The magnitudes of $\log_{10} ft$ fall roughly into groups corresponding to the forbiddenness of the transition as determined by the selection rules imposed by the nuclear matrix elements.

The Beta-Gamma Directional Correlation

Four of the first-forbidden beta decay nuclear matrix elements listed in Table 3 are operative for a spin change of one unit between initial and final nuclear states connected by the beta transition. These are $\int \bar{\sigma} \times \bar{r}$, $\int \bar{\alpha}$, $\int \bar{r}$, and $\int B_{ij}$. The matrix element $\int \bar{\alpha}$ may be expressed in terms of $\int \bar{r}$ through the nuclear matrix element parameter T

defined by Ahrens and Feenberg (38).

$$\Upsilon\zeta \int \bar{r} = - i \int \bar{\alpha} \ .$$

Here $\zeta = \alpha Z/2R$, where R and Z represent the radius and atomic number, respectively, of the daughter nucleus, and α is the fine structure constant. All observables other than the $\log_{10}$ft value depend only on ratios of the several nuclear matrix elements. It is convenient to express the other matrix elements in terms of the matrix element $\int B_{ij}$. We define two other independent nuclear matrix element parameters, x and u, in notation adapted from Kotani (13).

$$u = \frac{i \int \bar{\sigma} \times \bar{r}}{\int B_{ij}}$$

$$x = - \frac{C_V}{C_A} \frac{\int \bar{r}}{\int B_{ij}}$$

C_V/C_A is the ratio of vector to pseudovector coupling constants which determine the strength of the beta decay interaction.

A first-forbidden beta-gamma directional correlation $N(\theta)$ is conventionally expressed as

$$N(\theta) = 1 + A_2 P_2(\cos \theta),$$

where $P_2(\cos\theta)$ is the second-order Legendre polynomial. The formulas of Morita and Morita (17) result in the following expression for the A_2 coefficient:

$$A_2 = \frac{\sum_{\lambda \leq \lambda'} b_{\lambda\lambda'}(2)\ W(J_1, J_1, \lambda, \lambda'; 2, J_0)}{\sum_{\lambda \leq \lambda'} b_{\lambda\lambda'}(0)\ W(J_1, J_1, \lambda, \lambda'; 0, J_0)} \ \frac{G_2(\gamma)}{G_0(\gamma)} .$$

For a gamma transition containing a mixture of M1 and E2 radiations, the gamma factor is given by

$$\frac{G_2(\gamma)}{G_0(\gamma)} = \frac{F_2(1,1,J_2,J_1) + 2\delta\ F_2(1,2,J_2,J_1) + \delta^2\ F_2(2,2,J_2,J_1)}{1 + \delta^2} ,$$

where the angular correlation coefficients $F_2(L, L', J_2, J_1)$ are combinations of Clebsch - Gordon coefficients and Racah coefficients which are tabulated by Siegbahn (1). The gamma multipole mixing ratio δ is the ratio of the reduced matrix element for an E2 gamma transition to that for an M1 gamma transition. J_0, J_1, and J_2 are the spins of the initial, intermediate, and final nuclear states, respectively. The index λ or λ' represents the spherical tensor rank of the operative nuclear matrix elements and may assume values of 0, 1, or 2 for a first-forbidden beta transition. The parameters $b_{\lambda\lambda'}$ depend on the electron energy W and momentum P, on the neutrino momentum K, and on the nuclear matrix element parameters Υ, x, and u. For a first-forbidden beta transition where $|J_0 - J_1| = 1$, the index λ is limited to be either 1 or 2, and the parameters $b_{\lambda\lambda'}$ are as follows (17):

$$\frac{b_{11}(0)}{-2\sqrt{3}} = x^2\left(\frac{1}{3}K^2S_1 - \frac{2}{3}KS_3 + 2S_2 + S_4 + \zeta^2\Upsilon^2S_1 - \frac{2}{3}\zeta\Upsilon KS_1 + 2\zeta\Upsilon S_3\right) + u^2\left(\frac{1}{6}K^2S_1 + \frac{2}{3}KS_3 + \frac{1}{2}S_2 + S_4\right) + 2xu\left(\frac{1}{3}\zeta\Upsilon KS_1 + \zeta\Upsilon S_3 - S_2 + S_4\right)$$

$$b_{22}(0) = \frac{\sqrt{5}}{2}\left(\frac{1}{3}K^2S_1 + 3S_2\right)$$

$$\frac{b_{11}(2)}{-2\sqrt{6}} = 2x^2\left(\frac{1}{3}KS_5 - \frac{1}{2}S_2 - S_6 - \zeta\Upsilon S_5\right) + u^2\left(\frac{1}{3}KS_5 - \frac{1}{4}S_2 + S_6\right) + xu\left(\zeta\Upsilon S_5 - KS_5 + S_2 - S_6\right)$$

$$\frac{b_{12}(2)}{2} = x\left(3\zeta\Upsilon S_5 - KS_5 - 3S_2 + 3S_6\right) + u\left(KS_5 + \frac{3}{2}S_2 + 3S_6\right)$$

$$b_{22}(2) = -\frac{3}{2}\left(\frac{7}{2}\right)^{\frac{1}{2}}S_2$$

The parameters S_1 through S_6 are dependent on wave functions representing the emitted beta ray. They are given explicitly by Morita and Morita, denoted as L_0, L_1, N_0, M_0, L_{12}, and N_{12}, respectively (17). These parameters depend on the electron functions tabulated by Bhalla and Rose who made exact numerical solutions of the Dirac equation for a nuclear charge distribution of finite extent (15). Also given explicitly are the approximate expressions for S_1 through S_6 in the limit that $(\alpha Z)^2 \ll 1$. This ap-

proximation is used to obtain the formulas of Kotani with his parameters λ_1 equated to unity (13).

The beta energy spectrum shape correction factor C(W) is given by

$$C(W) = \frac{-b_{11}(0)}{\sqrt{3}} + \frac{b_{22}(0)}{\sqrt{5}} ,$$

or

$$C(W) = -\sqrt{10} \sum_{\lambda \leq \lambda'} b_{\lambda\lambda'}(0)\ W(J_1, J_1, \lambda, \lambda'; 0, J_0).$$

APPENDIX C

ANALYSIS OF EXPERIMENTAL DATA

APPENDIX C

ANALYSIS OF EXPERIMENTAL DATA

The largest correction required in the analysis of the beta-gamma coincidence data was the subtraction of accidental coincidences due to the finite resolving time of the coincidence circuit. The resolving time was determined by measuring the accidental coincidence counting rate by inserting a 0.4 microsecond time delay in the beta channel. This method of determining the resolving time was checked by the two-source technique. The gamma detector was removed and shielded from the Sb^{125} source. Then a separate Sb^{125} source was used to reproduce the observed gamma counting rate in the gamma detector, and the accidental coincidence counting rate was again measured. These two sources had no real coincidences. Therefore, this technique gave the correct measurement of the resolving time. Furthermore, the beta channel and the gamma channel were each operating at the same rate and under the same conditions as in the actual experiment.

A correction must be made, in general, for the gamma-gamma coincidence background. The magnetic quadrupole lens was used in this experiment to eliminate the need for this correction. The gamma-gamma coincidence background was measured, as discussed in Chapter IV, and was found to be negligible. Neither was any correction required for the decay of the radioactive source because all counting times were short compared to the 2.7 year half-life of Sb^{125}.

Table 4 gives experimental data for the directional correlation of beta rays in the energy range 0.235 - 0.275 MeV and the 0.176 MeV gamma ray. The analysis of these data to obtain one A_2 coefficient plotted on the graph of Figure 8 is outlined. The following notation is established for explanation of the analysis in six steps:

N_1 and N_2 represent the beta and gamma counting rates, respectively, when counting real plus accidental coincidences.

C_{r+a} represents the measured real plus accidental coincidence counting rate.

N_1' and N_2' represent the beta and gamma counting rates, respectively, when counting accidental coincidences.

C_a' represents the measured accidental coincidence counting rate.

C_a represents a calculated accidental coincidence counting rate.

C_r represents a calculated real coincidence counting rate.

1. The coincidence circuit resolving time τ is calculated for each run measuring the accidental coincidence counting rate.

$$\tau = \frac{1}{2} \frac{C_a'}{N_1' N_2'}$$

These calculations are averaged over several runs to yield τ_{av}.

2. The accidental coincidence counting rate C_a is calculated for each run measuring the real plus accidental coincidence counting rate C_{r+a}.

$$C_a = 2 N_1 N_2 \tau_{av}$$

Table 4. Analysis of Data for the Directional Correlation of Beta Rays in the Energy Range 0.235 - 0.275 MeV and the 0.176 MeV Gamma

Angle θ	Counting Time Hours	Total Coinc. C_{r+a}	Beta Count $\times 10^3$ N_1	Gamma Count $\times 10^5$ N_2	Beta-Gamma Product N_1N_2	Accid. Coinc. C_a'	Resolving Time Nanosec. τ	Accid. Coinc. C_a	Real Coinc. C_r	Norm. Real Coinc. C_r/N_1N_2
90	2	1825	648	343	2223			325	1500	6748
90	2		650	343	2230	310	50			
180	2	2039	623	348	2168			317	1722	7943
270	2	1824	623	343	2137			312	1512	7075
180	4	2041	618	348	2150			314	1727	8028
90	2	1724	643	344	2212			323	1401	6334
180	2	2007	624	349	2178			318	1689	7755
180	2		624	349	2178	331	55			
270	2	1835	625	344	2150			314	1521	7074
90	2	1744	625	344	2150			314	1430	6651
180	2	2008	618	349	2157			315	1693	7849
270	4	1748	616	344	2121			310	1438	6777
180	2	1972	637	349	2223			325	1647	7409
180	4		620	349	2163	318	53			
180	4	2040	618	349	2155			315	1725	8002
90	2	1774	619	344	2129			311	1463	6872

$$\eta = \frac{63016}{54308} = 1.160 \qquad A_2 = \frac{0.160}{1.580} = 0.1013 \qquad A_2(\text{corrected}) = \frac{A_2}{0.935} = 0.109$$

3. The real coincidence counting rate C_r is calculated for each run measuring the real plus accidental coincidence counting rate C_{r+a}.

$$C_r = C_{r+a} - C_a$$

4. Each real coincidence counting rate C_r is normalized to the product N_1N_2 of the beta and gamma counting rates. This normalization makes a first-order correction for small error in source centering and small drifts in the electronic circuits which affect the counting rates.

5. The anisotropy is defined as $\eta - 1$, where

$$\eta = \left(\frac{C_r}{N_1N_2}\right)_{180} \div \left(\frac{C_r}{N_1N_2}\right)_{90,270} .$$

Here $(C_r/N_1N_2)_{180}$ denotes data taken at the 180 degree counting position, and $(C_r/N_1N_2)_{90,270}$ denotes the average of data taken at the 90 degree and 270 degree counting positions.

6. The beta-gamma directional correlation $N(\theta)$ is expressed as

$$N(\theta) = 1 + A_2 P_2(\cos \theta) .$$

The A_2 coefficient is calculated from η as

$$A_2 = \frac{\eta - 1}{1 + \frac{\eta}{2}} .$$

The value of the A_2 coefficient calculated here represents the true A_2 coefficient averaged over the solid angles subtended by the two detectors. A solid angle correction was made, as discussed in Appendix D, to obtain the value $A_{2(\text{corrected})}$. This value is plotted in Figure 8. The statistical standard deviation in any large number of counts was assumed to be the square root of that number, and the probable statistical error accumulated in the calculation of the A_2 coefficient was obtained by the procedure derived by Beers (39).

APPENDIX D

ANGULAR RESOLUTION CORRECTION

APPENDIX D

ANGULAR RESOLUTION CORRECTION

The directional correlation $N(\theta)$ for two coincident radiations is expressed theoretically as the sum of a finite series of Legendre polynomials (1).

$$N(\theta) = \sum_{n} c_n P_n(\cos \theta) \ .$$

The experimental coincidence counting rate is proportional to $N(\theta)$ only in the limiting case of a centered point source and point detectors. We assume that a centered point source is well approximated in the laboratory and proceed to discuss the correction for the finite solid angles subtended at the source by the two detectors. Reference is made to Figure 16 illustrating the detector geometry. The detectors are scintillation crystals in the form of right circular cylinders. The source is positioned at the intersection of the axes of the cylinders.

The theoretical probability per unit time of two coincident radiations being detected simultaneously in differential solid angles $d\Omega_1$ and $d\Omega_2$ at a relative angle θ is proportional to $N(\theta)d\Omega_1 d\Omega_2$. The coincidence counting rate for two detectors positioned with their axes at a relative angle θ is proportional to

$$\iint N(\theta') \ \epsilon(\alpha_1) \ \epsilon(\alpha_2) \ d\Omega_1 d\Omega_2 \ ,$$

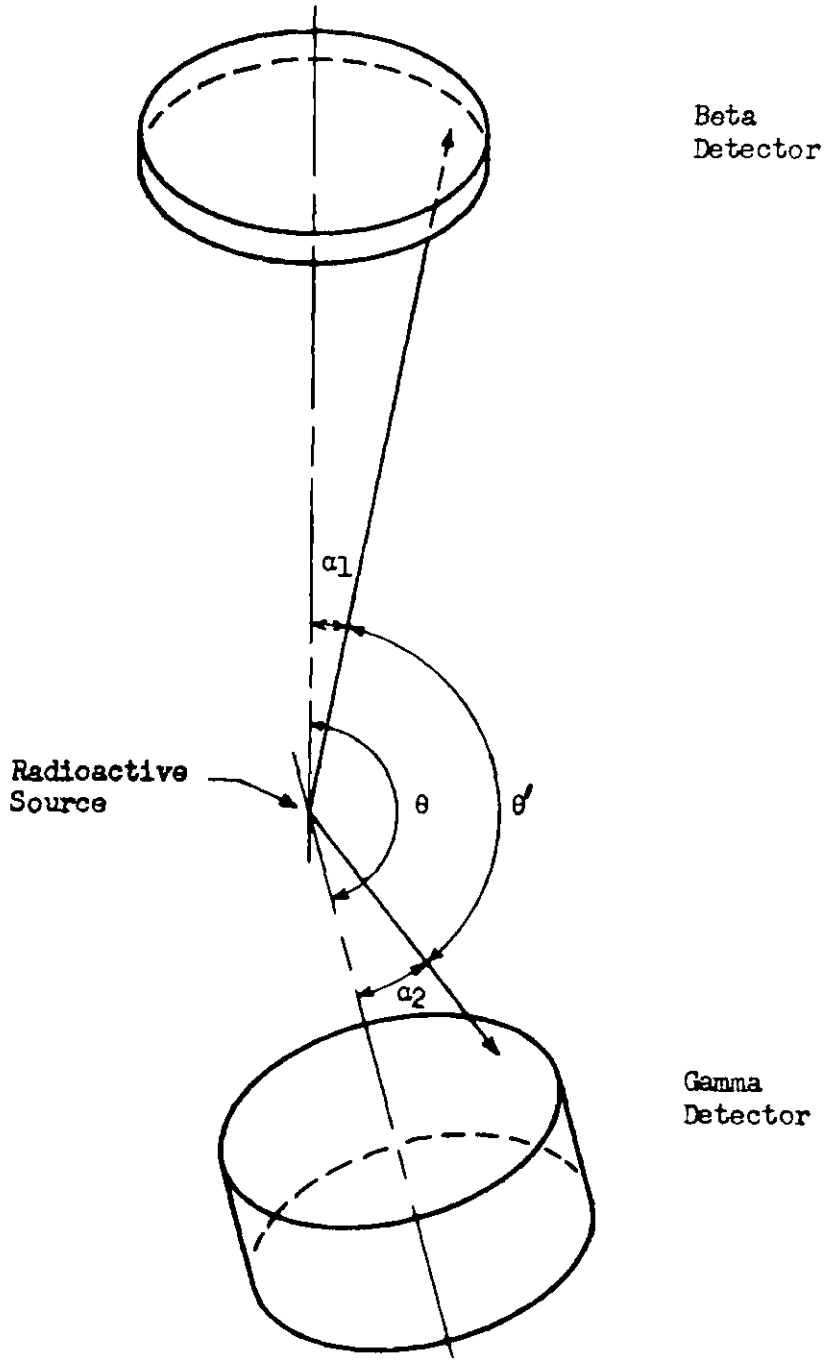

Figure 16. Geometry for Angular Resolution Correction.

where the integration proceeds over the solid angles subtended by the two detectors. The angle between the two coincident radiations is θ', and $\epsilon(\alpha)$ represents the detector counting efficiency for a radiation incident at an angle α relative to the axis of the detector. Then the measured directional correlation $N_m(\theta)$ is given by

$$N_m(\theta) = \frac{\iint N(\theta')\ \epsilon(\alpha_1)\ \epsilon(\alpha_2) d\Omega_1 d\Omega_2}{\iint \epsilon(\alpha_1)\ \epsilon(\alpha_2) d\Omega_1 d\Omega_2} \quad .$$

Rose has shown that the form of the directional correlation is unchanged by the solid angle correction, but each Legendre polynomial coefficient c_n is multiplied by a product of attenuation factors, $Q_n(1)Q_n(2)$, where $Q_n(i)$ is due to the finite size of detector i (40). Q_n is given by $\frac{J_n}{J_o}$, where

$$J_n = \int_o^{\alpha_{max}} P_n(\cos\alpha)\ \epsilon(\alpha)\ \sin\alpha\ d\alpha \quad .$$

For the beta scintillation detector, $\epsilon(\alpha)$ is approximately unity. Then

$$Q_2 = \frac{1}{2} \cos\alpha_{max}\ (1 + \cos\alpha_{max}) \quad .$$

The effective solid angle subtended by the beta detector was determined by comparing the counting rate with that for a simple geometry, as discussed in Chapter III, with the result that $Q_2 = 0.995$.

For the gamma scintillation detector, Rose has used the approxima-

tion that any gamma ray which interacts with the crystal is counted in the total absorption peak (photopeak) (40). Then

$$\epsilon(\alpha) = 1 - \exp(-\tau x) ,$$

where τ is the linear absorption coefficient for a gamma ray traversing thickness x of the crystal. Stanford and Rivers have calculated values of Q_2 based on this approximation (41). Yates has limited $\epsilon(\alpha)$ to be the actual photopeak efficiency, using Monte Carlo calculations to obtain Q_2 (42). The curves of either Yates or Stanford and Rivers give a value of 0.94 for Q_2 for 0.176 MeV gamma rays incident upon a 1-1/2 inch diameter by one inch thick NaI(Tl) crystal six centimeters from the source. The corrected A_2 coefficients listed in Table 2 were obtained by dividing the experimentally determined A_2 coefficients by

$$Q_2(1)Q_2(2) = 0.935.$$

BIBLIOGRAPHY

1. H. Frauenfelder and R. M. Steffen, Angular Correlations, in Alpha-, Beta-, and Gamma-Ray Spectroscopy (ed. K. Siegbahn): North-Holland Publishing Company, Amsterdam, 1965.

2. D. R. Hamilton, Physical Review, 58 (1940) 122.

3. E. L. Brady and M. Deutsch, Physical Review, 72 (1947) 870.

4. H. Frauenfelder, Annual Review of Nuclear Science, 2 (1953) 129.

5. L. C. Biedenharn and M. E. Rose, Reviews of Modern Physics, 25 (1953) 729.

6. E. J. Konopinski and G. E. Uhlenbeck, Physical Review, 60 (1941) 308.

7. T. D. Lee and C. N. Yang, Physical Review, 104 (1956) 254.

8. C. S. Wu, E. Ambler, R. W. Hayward, D. D. Hoppes, and R. P. Hudson, Physical Review, 105 (1957) 1413.

9. E. J. Konopinski, Annual Review of Nuclear Science, 9 (1959) 99.

10. H. A. Weidenmüller, Reviews of Modern Physics, 33 (1961) 574.

11. M. A. Preston, Physics of the Nucleus: Addison-Wesley Publishing Company, Reading, Massachusetts, 1962.

12. T. Kotani and M. Ross, Physical Review, 113 (1959) 622.

13. T. Kotani, Physical Review, 114 (1959) 795.

14. R. W. Newsome, Jr. and H. J. Fischbeck, Physical Review, 133B (1964) 273.

15. C. P. Bhalla and M. E. Rose, Oak Ridge National Laboratory Report, ORNL-3207 (1961).

16. C. P. Bhalla and M. E. Rose, Physical Review, 128 (1962) 774.

17. M. Morita and R. S. Morita, Physical Review, 109 (1958) 2048.

18. M. G. Mayer and J. H. D. Jensen, Elementary Theory of Nuclear Shell Structure: John Wiley and Sons, New York, 1955.

BIBLIOGRAPHY (Continued)

19. S. B. Burson, J. M. LeBlanc, and D. W. Martin, Physical Review, 105 (1957) 625.

20. A. Arya and N. Nicholson, Bulletin of the American Physical Society, 11 (1966) 67.

21. K. Siegbahn and W. Forsling, Arkiv för Fysik, 1 (1950) 505.

22. J. Moreau, Arkiv för Fysik, 7 (1954) 391.

23. N. H. Lazar, Physical Review, 102 (1956) 1058.

24. G. Chandra and V. R. Pandharipande, Nuclear Physics, 46 (1963) 119.

25. R. S. Narcisi, Harvard Technical Report, 2-9 (1959); AECU-4336 (1959).

26. Nuclear Data Sheets, National Academy of Sciences--National Research Council, (National Research Council, Washington, D. C.)

27. G. R. Fowles, Physical Review, 76 (1949) 571; 78 (1950) 744.

28. J. S. Geiger, R. L. Graham, I. Bergström, and F. Brown, Nuclear Physics, 68 (1965) 352.

29. S. A. Moszkowski, Theory of Multipole Radiation, in Alpha-, Beta-, and Gamma-Ray Spectroscopy (ed. K. Siegbahn): North-Holland Publishing Company, Amsterdam, 1965.

30. T. Inamura, T. Iwashita, Y. Ikemoto, and S. Kageyama, Journal of the Physical Society of Japan, 19 (1964) 239.

31. M. E. Rose, Internal Conversion Coefficients: North-Holland Publishing Company, Amsterdam, 1958.

32. W. Weidemann, Nuclear Instruments and Methods, 9 (1960) 347.

33. H. A. Enge, Review of Scientific Instruments, 30 (1959) 248.

34. J. P. Blewett, Brookhaven National Laboratory Report, BNL-4654 (1959).

35. N. K. Glendenning, Physical Review, 119 (1960) 213.

36. A. J. Rassey, Physical Review, 109 (1958) 949.

37. B. R. Mottelson and S. G. Nilsson, Det Kongelige Danske Videnskabernes Selskab, Matematisk-Fysiske Skrifter, 1 (1959) No. 8.

BIBLIOGRAPHY (Concluded)

38. T. Ahrens and E. Feenberg, Physical Review, 86 (1952) 64.

39. Y. Beers, Introduction to the Theory of Error: Addison-Wesley Publishing Company, Reading, Massachusetts, 1958.

40. M. E. Rose, Physical Review, 91 (1953) 610.

41. A. L. Stanford and W. K. Rivers, Review of Scientific Instruments, 30 (1959) 719.

42. M. J. L. Yates, Finite Solid Angle Corrections, in Alpha-, Beta-, and Gamma-Ray Spectroscopy (ed. K. Siegbahn): North-Holland Publishing Company, Amsterdam, 1965.

43. J. Fujita, Physical Review, 126 (1962) 202.

44. J. Eichler, Zeitschrift für Physik, 171 (1963) 463.

VITA

James Leroy DuBard was born in Atlanta, Georgia, on March 13, 1937. He attended Morningside School and Henry Grady High School in Atlanta. He entered Georgia Institute of Technology in 1955 and graduated with the B.S. degree, with honor, in electrical engineering. He was elected to Who's Who in American Colleges and Universities. He began graduate study in electrical engineering at Massachusetts Institute of Technology in 1959 and received the M.S. degree two years later. During this time he held a full-time research assistantship in the High Voltage Engineering Laboratory. A third year at M.I.T. was devoted to the undergraduate physics core curriculum. In 1962, he began graduate study in physics at Georgia Institute of Technology, where he held a NASA fellowship for three years. He is a member of Sigma Chi Fraternity, Sigma Pi Sigma, and Sigma Xi. He is married to the former Mary Clayton Bryan of Charlotte, North Carolina. They have a son and a daughter.